Centre for Geo-Information

Thesis Report GIRS-2015-04

Pan-tropical analysis of deforestation drivers using global land cover products and the role of deforestation drivers in global gross carbon emissions for 1990-2000-2005 time period

Simon Besnard

February 2015

© CIFOR

WAGENINGEN UNIVERSITY
WAGENINGEN UR

Pan-tropical analysis of deforestation drivers using global land cover products and the role of deforestation drivers in global gross carbon emissions for 1990-2000-2005 time period

Simon Besnard

Registration number 860314-060-060

Supervisors:

Veronique De Sy, MSc., Laboratory of Geo-information Science and Remote Sensing, Wageningen University
Prof. Dr. Martin Herold, Laboratory of Geo-information Science and Remote Sensing, Wageningen University

A thesis submitted in partial fulfilment of the degree of Master of Science
at Wageningen University and Research Centre,
The Netherlands.

Date: February 26, 2015
Wageningen, The Netherlands

Thesis code number: GRS-80436
Thesis Report: GIRS-2015-04
Wageningen University and Research Centre
Laboratory of Geo-Information Science and Remote Sensing

Foreword and Acknowledgements

My passion for studying natural resource management and climate change has its roots back home, in France where I started my career when I was around 8 years old, as a kind of apprentice at my uncle's farm. I remember the weekends I spent during my childhood, learning how to farm but also listening to my uncle talking about the importance of good land management practices year after year and how climate change was impacting the agricultural productivity of his land. Therefore, I developed an undying interest to understanding the role of anthropogenic interventions on natural resource and climate change The thesis presented is a product of this funded interest and a continuity of my on-going personal-professional exploration.

As a result, I would like to first thank my family, in particular my parents who with their joint and separate example have inspired me to pursue my own dreams. Without their education and the multiple sacrifices they undertook to give me the best education, I would have certainly not arrived at this point.

I also want to give a special thanks to my supervisors Niki De Sy and Martin Herold for their guidance and advice during my research. I really appreciate the fact that they gave me important inputs as well as a lot freedom for developing my own methodology. Niki and Martin, thank you very much for your dedicated support all the way!

This research would have never been possible without the FRA2010 datasets provided by the FAO. I am also grateful to the CCI land cover team, the MODIS land team and the FAO for providing the global land cover maps, as well as to the global forest biomass producers whom allowed me to undertake the carbon emissions analysis. Special thanks to Gregory Asner and his team at the Carnergie Institution for Science for releasing these amazing high-resolution carbon maps of Peru and Colombia. I would like to especially thank the open source community for providing most of the tools I used during my thesis, in particular R, RStudio as well as Robert Hijmans, Roger Bivand, Edzer Pebesma and Hadley Wickham for their raster, rgdal, sp and ggplot2 packages, respectively.

I am also greatly indebted with Valerio Avitabile who gave me a lot of advice to carry out the carbon emissions analysis. Special thanks to Loïc Dutrieux for listening to my issues with the datasets and helping me with the R programming. Loïc, I owe you quite a lot of *La Chouffe* beers! I also would like to thank my Wageningen friends and my housemates from Heerenstraat 14 for their encouragement, cooking and forced distractions that made this thesis less stressful. Finally, I want to thank all my fellow MGI master students for sharing the thesis room daily and drinking litres of coffee for the last six months with me.

Abstract

Tropical deforestation is considered the second largest source of anthropogenic greenhouse gas emissions. Consequently, there is a need to identify land use change and forestry activities - in particular those that are linked to the drivers of deforestation and forest degradation - and to assess their potential contribution to the mitigation of climate change. In this study, we aimed to (i) assess the suitability of global land cover maps for deforestation drivers' analysis and (ii) to analyse gross carbon emissions per driver using sample-based driver data and global forest biomass maps in the pan-tropical region for the 1990-2005 time period. First, our study assessed three global land cover maps for deforestation drivers' classification in Africa and South America: Modis500, CCI-LC and GLC-SHARE land cover maps. We showed that there are opportunities to use global land cover maps for deforestation drivers' analysis, in particular with the CCI-LC product in the two continents. The estimated overall accuracies of the CCI-LC products were 60% and 90% in Africa and South America, respectively. User and producer's accuracies for each driver class were also reported. We concluded that the CCI-LC product could be used for the agriculture driver classification in both continents although this product will overmap agriculture class in Africa- i.e. low user accuracy. Second, we estimated carbon losses per driver in South America for the 1990-2005 time period based on the 2010 global remote sensing survey of the FRA2010 and the deforestation drivers classification dataset. Forest cover changes per driver were combined with Yong *et al.* (2014) pan-tropical biomass map to estimate carbon losses. The method was validated with high-resolution carbon maps for both Colombia and Peru. We showed that there were gross carbon losses from deforestation of 195±4.2 $MtC.yr^{-1}$ and 246±4.9 $MtC.yr^{-1}$ for the 1990s and the 2000s, respectively. Agriculture account for circa 90% of the total carbon emissions for the two periods. Our study also demonstrated that circa 80% of the carbon losses from deforested occurred in the tropical rainforest ecosystem. Our estimates of carbon losses from deforestation are significantly lower compared to earlier published estimates.

Keywords: Climate change, tropical deforestation, deforestation drivers' classification, global land cover maps, carbon emissions from deforestation, pantropical biomass maps.

Table of Contents

List of figures

List of tables

Abbreviations

AD	Activity Data
AFOLU	Agriculture, Forestry and Other. Land Use
AGB	Aboveground Biomass
CCI	Climate Change Initiative
CE	Carbon Emission
CIFOR	Centre for International Forestry Research
COP	Conference of the Parties to the UNFCCC
EF	Emission Factor
FAO	Food and Agriculture Organization of the United Nations
FRA	Forest Resource Assessment
GHG	Greenhouse Gas
GCS REDD+	Global Comparative Study on REDD+
GOFC-GOLD	Global Observation of Forest and Land Cover Dynamics
GLC	Global Land Cover
GPG	Good Practice Guidance
IPCC	Intergovernmental Panel on Climate Change
LiDAR	Light Detection and Ranging
LCCS	Land Cover Classification System
LUC	Land-Use Change
LUCS	Land Use Classification System
MMU	Minimum Mapping Unit
MODIS	Moderate Resolution Imaging Spectroradiometer
MRV	Measurement, Reporting and Verification

REDD+	Reducing emissions from deforestation and forest degradation in developing countries; and the role of conservation, sustainable management of forests and enhancement of forest carbon stocks in developing countries
RSS	Remote Sensing Survey
UNFCCC	United Nations Framework Convention on Climate Change
UN-REDD	The United Nations Collaborative Programme on Reducing Emissions from Deforestation and Forest Degradation in Developing Countries
WHRC	Wood Hole Research Centre

Chapter 1. Introduction

Tropical deforestation is considered the second largest source of anthropogenic greenhouse gas (GHG) emissions (IPCC, 2007) and is expected to remain a major emission source for the future (MEA, 2005). Despite relevant efforts to reduce deforestation, around 13 million hectares of forests is lost every year (FAO, 2010). The reduction of GHG emissions from tropical deforestation is now recognized as an essential component of international efforts to mitigate climate change. Reducing emissions from deforestation and degradation whilst simultaneously enhancing the carbon stock of tropical forests (REDD+) is seen as leverage for mitigating climate change. REDD+ initiatives aimed at implementing national measurement, reporting and verification (MRV) systems according to the international Good Practice Guidelines (GPG) of the intergovernmental Panel on Climate Change (IPCC) (GOFC-GOLD, 2010). This includes estimating and monitoring changes of both the area of deforestation and degradation, and the terrestrial carbon stock densities per unit area (IPCC, 2006).

1.1. Background information

One of the key inputs into the IPCC framework is the carbon stocks of the forests undergoing change. In order to estimate the magnitude of carbon emissions from deforestation two variables have to be determined. The difference between the pre- and post- deforestation or degradation carbon stocks is the emission factors (EFs), which are the carbon emissions per unit area due to forest cover change. The product of the EF and the area of forest change, also called Activity Data (AD), provides the estimate of the total carbon emissions (IPCC, 2006). These two variables are the most important components to estimate carbon emissions, no matter the approach used (Houghton, 2012). That is why the UNFCCC negotiations (UNFCCC, 2009; 2010) have encouraged annexe I countries to identify land use, land use change and forestry activities, in particular those that are linked to the drivers of deforestation and forest degradation, and to assess their potential impact to climate change (Hosonuma *et al.*, 2012).

Deforestation and forest degradation are caused by multiple drivers and pressures, including proximate/direct- and underlying/indirect- causes. Proximate causes are human activities or immediate actions that directly impact forest cover and loss of carbon; conversely, underlying drivers are based on a synergy of multiple factors driven by economic, institutional, technological, cultural, and demographic variables (Geist and Lambin, 2002). Direct drivers can be grouped into different categories such as commercial and subsistence agriculture, mining, infrastructure extension and urban expansion (Kissinger *et al.*, 2012). Rademaekers *et al.* (2010) stated that there is rarely a single direct or indirect driver responsible for deforestation but, most often, multiple processes work simultaneously or sequentially causing deforestation.

The need for data on drivers and activities causing forest carbon change is relevant not only for assessing deforested areas but is also fundamental for the development of policies and measures, such as REDD+ (Boucher, 2011; UNFCCC, 2010). Nevertheless, quantitative national-level information on drivers and activities causing deforestation and forest degradation are widely unknown (Houghton, 2012). In addition, Hosonuma *et al.* (2012) stated that the fraction of deforestation in a country caused by a specific driver (e.g. agriculture expansion vs. infrastructure) cannot be answered for many developing countries.

One of the reasons is that previous studies (Geist and Lambin 2001) have mainly been based on local-scale studies or regional to global assessments (De Fries *et al.*, 2010, Boucher *et al.*, 2011). In addition, some studies (Kissinger *et al.*, 2012) gave insights on drivers that lead to deforestation and forest degradation at continental scale. The synthesis showed that agriculture is the most significant driver of deforestation, but with differences in terms of geographical distribution and magnitude between commercial and subsistence agriculture, followed by infrastructure development and wood extraction. Growing populations of shifting cultivators and smallholders used to be considered as the main driver of deforestation and forest degradation. Kissinger *et al.* (2012) and Boucher *et al.* (2011) have also shown that commercial actors currently play a larger role in the expansion of agriculture into forests, in particular agribusinesses linked to international markets (Rudel *et al.*, 2009).

High GHG emissions from deforestation and forest degradation mostly occur in the tropical regions, where forest carbon density is the highest (Baccini *et al.*, 2012). Therefore, quantifying the roles of forests as carbon stores, sources of carbon emissions and carbon sinks has become one of the key factors to understanding the global carbon cycle (FAO, 2010, Canadell *et al.*, 2007). That is why the Kyoto Protocol and the UNFCCC request all member countries to assess and report national GHG emissions regularly, including emissions and removals of carbon reflected as stock changes in forests (UNFCCC, 2009). In order to estimate carbon stock, one approach is to map vegetation types within a landscape and assign a carbon density value to each vegetation type, using either international or locally-derived values from field based inventory (GOFC-GOLD, 2009). The IPCC has developed guidelines, methods and default values for the parameters needed to assess carbon stocks and their changes in forests (IPCC, 2006), including both carbon emissions and removals. It has therefore provided all countries with the means of estimating and reporting carbon stocks, greenhouse gas emissions and removals. However, this method can have high uncertainty, especially at global scale or when using default carbon density values (Mitchard *et al.*, 2013).

Recently, efforts have been made to quantify the amount of carbon stored in Aboveground Biomass (AGB) in the pan-tropical region, but most of the time with high uncertainties (Baccini *et al.*, 2012; Houghton *et al.*, 2012). Salimon *et al.* (2011) stated that biomass estimation methods range from ground-based and site specific to remotely sensed and global (e.g. Achard *et al.*, 2014; Baccini *et al.*, 2012, Harris *et al.*, 2012; FAO, 2010; Saatchi *et al.*, 2011; Chave *et al.*, 2005; GOFC-GOLD, 2009). Quantifying emissions from deforestation has largely made use of simple book-keeping models based around FAO and IPCC data (Morton *et al.*, 2009; IPCC, 2007) and, more recently, explicit forest biomass maps to quantify carbon stocks before deforestation at a pixel level (Harris *et al.*, 2012). The Global Forest Resources Assessment (FRA) published by the FAO provides a comprehensive accounting of AGB carbon stocks for tropical forests and other wooded lands. The FRA 2010 (FAO, 2010) estimates are derived from national forest inventories. Additionally, Baccini *et al.* (2012) estimated the CO_2 emissions from tropical deforestation for the period 2000-2010 using satellite derived biomass, satellite-derived biomass weighted by deforestation and FRA 2010 biomass. In addition, Houghton (2012) provided a review of the link between carbon emissions and deforestation drivers at global scales. The study showed that shifting cultivation is of greatest importance over the period 1990-2009 while the conversion of forests to permanent croplands in the tropics was responsible for the second largest emissions of carbon. Conversely, Tubiello *et al.* (2015) showed that crop and livestock activities have become the dominant source of AFOLU emissions. This study also highlighted the large

uncertainties that characterize emission estimates in the AFOLU sector; therefore quantification of AFOLU emission sources and sinks still remains uncertain, even at global scale (Tubiello *et al.*, 2015).

1.2. Problem statement

Understanding drivers of deforestation and their importance are relevant for the development of policies and measures that aim to alter current trends in forest activities toward a more climate and biodiversity friendly outcome (Hosonuma *et al.*, 2012). However, the availability of data on drivers remains uncertain in many REDD+ countries (Kissinger *et al.*, 2012). So far, analyses of drivers have largely been based on local or regional case studies (Geist and Lambin, 2002) or on coarser assessments on the continental and global scales (DeFries *et al.*, 2010, Rademaekers *et al.*, 2010). Spatial assessments of proximate deforestation drivers based on remote sensing techniques and ground data have recently become available that allow for a more comprehensive assessment of the deforestation drivers in the pan-tropical region (FAO, 2010; ongoing work of Veronique De Sy). Nevertheless, the existing imagery is, in some regions, not sufficient to assess follow-up land use due to low resolution and/or cloud cover. Therefore, the use of existing global land cover maps might provide an alternative source of information to overcome this issue.

Furthermore, the types of drivers of deforestation have great influence on the forest carbon impacts and the choice of data sources and methods used to measure and monitor them (Kissinger *et al.*, 2012). Although carbon emissions from fossil fuel use are relatively well quantified, emissions from LUC are the most uncertain component of the global carbon cycle (Harris *et al.*, 2012). Large uncertainties in emission estimates arise from inadequate data on the carbon density of forests (Houghton *et al.*, 2012; Baccini *et al.*, 2012). Currently the carbon stocks for a region or country are often based on guideline mean biomass values for particular vegetation types (IPCC, 2003) or on country-specific mean carbon stock values, i.e. FRA 2010 (FAO, 2010). That is why Mitchard *et al.* (2013) suggests that pantropical biomass maps can provide much better estimates of carbon stocks at a project or national level. Additionally, little is known yet on the link between carbon emissions and deforestation drivers because there are information gaps in the follow-up land use after deforestation (Kissinger *et al.*, 2012; Harris *et al.*, 2012). This implies that there is a need to have robust and complete deforestation driver data to generate a gross emission estimate per driver. Therefore, sample-based deforestation driver data combined with wall-to-wall biomass data can be integrated to estimate carbon changes and gross carbon emissions per deforestation's driver.

1.3. Research objectives

Given the current gap in knowledge and understanding of drivers on national, regional and global levels and the link between carbon emissions and drivers, the overall objectives of this thesis are to develop approaches to (i) overcome the lack of information on deforestation drivers and to (ii) estimate the gross carbon emissions related to each drivers in (sub)tropical non-annex 1 countries. The thesis is set out to:

- Assess the suitability of global land cover data to improve the deforestation driver's analysis in the pan-tropical region; and
- Analyse gross carbon emissions per driver at tile, country, regional and continental scales using sample-based driver data and global forest biomass maps in the pan-tropical region.

In the following pages the report of the thesis is presented. Chapter 2 describes all data sets used and presents the methodology developed to analyse the data. Results for the accuracy assessment of the global land cover maps are described and discussed in Chapter 3. Results for the carbon emissions analysis are presented in Chapter 4 including comparison of the results with other studies. Finally, some conclusions and recommendations are given in Chapter 5 for future research.

Chapter 2. Material and methods

2.1. Assessment of global land cover maps for deforestation drivers analysis

The assessment of the global land cover maps for the deforestation drivers' analysis in the pan-tropical region was carried out for two epochs: 1990-2000 and 2000-2005. The accuracy assessment was done both in Africa- including Southern Africa, Eastern Africa and Central Africa - and in South America. For the aim of the study, only the proximate/direct drivers were analysed. Also, only the drivers related to deforestation were included in our study because forest degradation is hard to detect, therefore it requires fine resolution optical imagery or LiDAR (Herold *et al.*, 2011) and is usually not reflected by a change in the land cover class (Achard *et al.*, 2014).

Figure 2.1 gives a general overview of the method, which was used for assessing the suitability of global land cover maps to analyse the deforestation drivers for the two epochs considered in this study, i.e. 1990-2000 and 2000-2005. The different steps of the methodology are detailed in the next sections. All developing steps were conducted in R (R Development Core Team 2013), supported by ArcGIS and Google Earth for visualization.

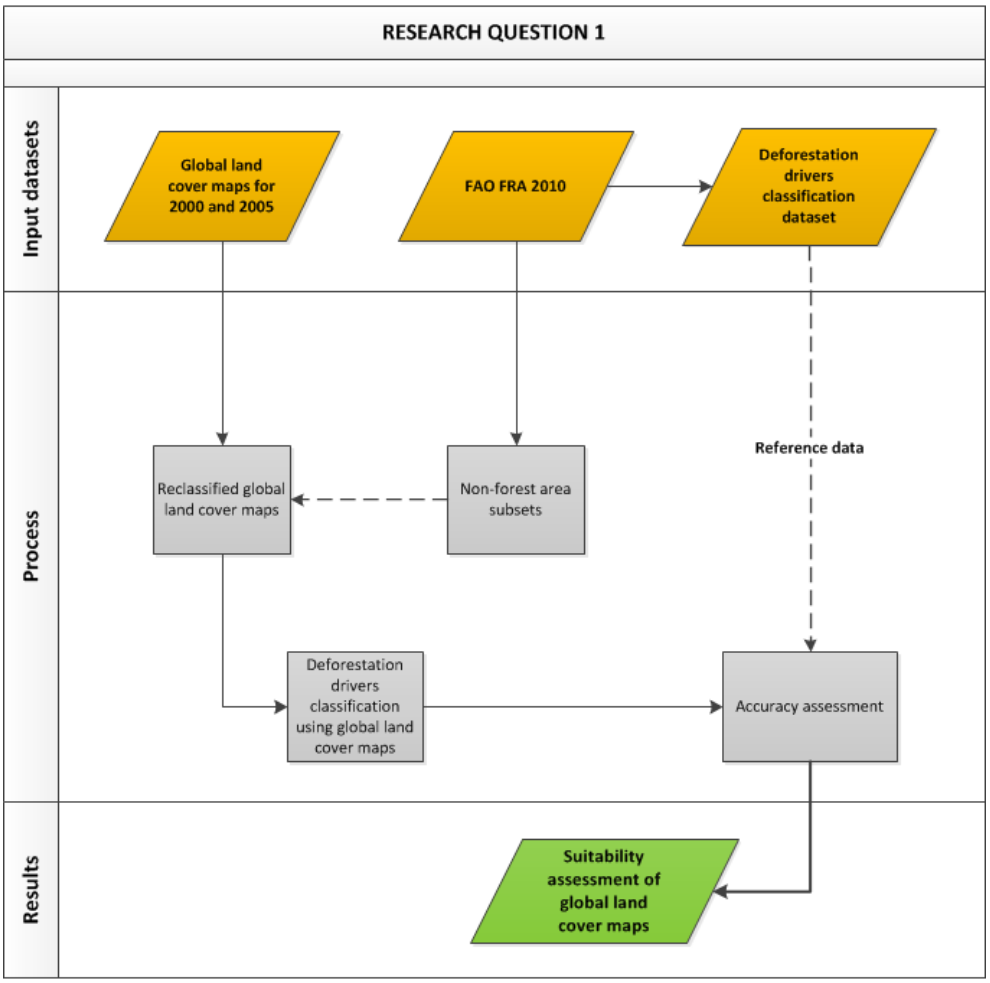

Figure 2.1: Flowchart of the method for deforestation drivers' classification assessment for 1990-2000-2005.

2.1.1. Data acquisition

This study aimed to assess three global land cover datasets for deforestation drivers classification: the CCI land cover map 2000-2005, GLC SHARE map, and the MODIS 500m land cover map 2000-2005. Table 2.1 below provides a description of the three global land cover maps considered in our study whilst table 2.2 compares several key indicators of these land cover maps.

Table 2.1: General overview of the land cover datasets. Source: adapted from Potere and Schneider (2007)

Code	Map	Producer	Specifications / Source
CCI-LC	Climate Change Initiative Land Cover	CCI-LC partnership	Global land cover map, raster, *http://www.esa-landcover-cci.org/?q=node/123*
GLC-SHARE	Global Land Cover SHARE	Food and Agriculture Organization of the United Nations (FAO)	Global land cover map, raster, *http://www.fao.org/geonetwork/srv/en/main.home?uuid=ba4526fd-cdbf-4028-a1bd-5a559c4bff38*
MOD500	MODIS Land Cover 500 m (Schneider et al., 2009)	University of Wisconsin and Boston University (US-NASA)	Global land cover, raster, *http://sage.wisc.edu/people/schneider/research/data_readme.html*

Table 2.2: Comparison of key indicators for each land cover maps. Source: adapted from Potere and Schneider (2007) and Kuenzer *et al.* (2014)

Code	*Spatial resolution*	*Time of data collection*	*Products and methods used*	*Classification scheme*	*Land cover classes*
CCI-LC	300m for 2005 and 2010 and 1000m for 2000	1998-2012	MERIS time series and spot VGT	FAO LCCS	22
GLC-SHARE	30 arc second (1,000m).	2000, 2009 and 2012	National or regional data, Globcover 2009, MODIS VCF 2010 and Cropland database 2012.	FAO LCCS	11
MOD500	463 m	2001-2011	Multi-spectral MODIS observations	IGBP	17

As reference data, our study used a deforestation drivers' classification dataset based on the ongoing work of Veronique De Sy. Her study is currently using the 2010 global remote sensing survey (RSS) of the FRA2010 to assess regionally specific deforestation drivers, by visual interpretation of forest change patches and follow-up land use in deforestation areas (FAO and JRC, 2012) using Landsat Global Land Survey datasets and Google Earth. The RSS global sampling grid consists of 13 689 sites and covers the globe between 75 degrees North and South in latitude (figure 2.2). A systematic sampling design based on each longitude and latitude intersection was implemented. Each sample tile covers a 10 by 10 kilometre square at every one-degree latitude and longitude junction (approximately 100 km apart) (FAO, 2009).

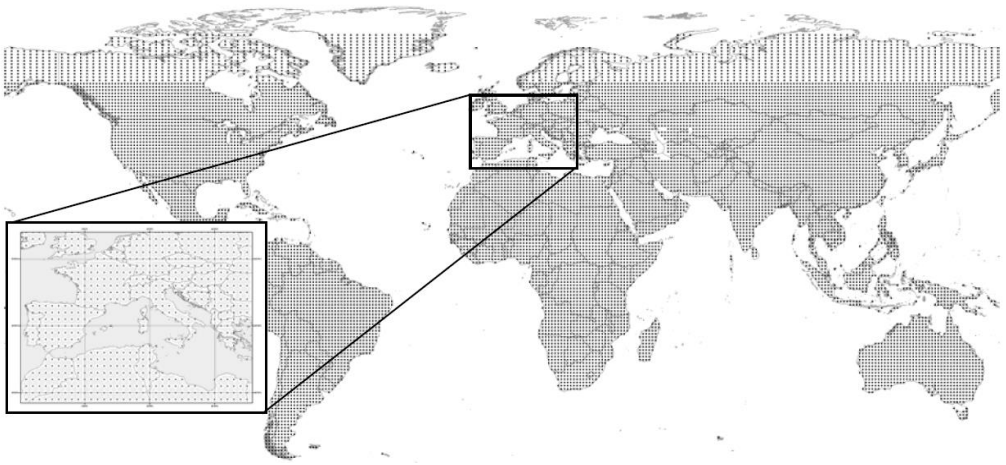

Figure 2.2: Distribution of the 13 689 FRA 2010 RSS global survey sites. Inset shows detail of sample sites across parts of Europe and North Africa. Source: FAO (2009)

Table 2.3 describes the deforestation drivers included in the deforestation drivers classification dataset.

Table 2.3: Drivers classification and codes. Source: Adapted from FAO (2010)

Main class (code)	**Sub-class (code)**	
Forest (100)		
Agriculture (200)	Crop agriculture (250)	Small-holder crop agriculture (210)
		Commercial crop agriculture (220)
	Tree crops (230)	
	Pasture / grazing land (240)	
Built-up (300)		
Mining (400)		
Other (500)	Other land with tree cover (520)	
	Grass and herbaceous (530)	
Water (600)		
No data (999)		

2.1.2. Reclassification of the global land cover maps

Forest definitions change from country to country based on national definitions, cultural values and the purpose of the assessment and the methodology used (FAO, 2010). In this study, the definition of forest provided by FAO was applied and was defined as land spanning more than 0.5 ha with more than 10% tree canopy cover and trees higher than 5 m (or having the potential to reach a height of 5 m) (FAO, 2000). In addition, table 2.2 shows that the three global land cover maps have different land cover classification systems. CCI-LC, GLC-SHARE and MODIS500 maps have 22, 11 and 17 different land cover classes, respectively. Therefore, we had to aggregate all classes to have a generalized global legend based on a set of common classifiers. Annexe 1 gives an overview of the land use/driver classification system which have been adapted from Kuenzer *et al.* (2014).

2.1.3. Accuracy assessment

The first step of the accuracy assessment was to undertake a deforestation drivers' classification using the global land cover maps and the 2010 global RSS of the FRA2010. Figure 2.3 illustrates the method we developed in order to classify the deforestation drivers. For the 1990-2000 and 2000-2005 time periods, our study was interested in determining what

the fate of the forest was both during the 1990s and the 2000s. The 2010 global RSS dataset allowed us to select the patches converted to non-forest land uses during the 1900s and the 2000s. Then, we were able to classify the follow-up land use after deforestation and see whether forest was converted either to cropland, grassland, wetlands, settlements, other land or remains forest by using the global land cover maps of 2000 and 2005.

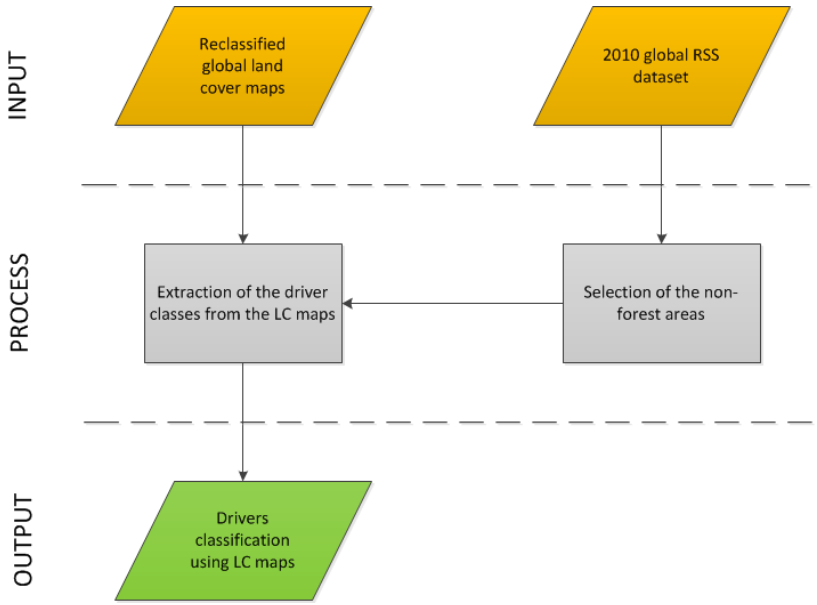

Figure 2.3: Classification process of the follow-up land use after a deforestation event using global land cover maps.

Once the deforestation drivers' classification was performed, we computed a confusion matrix for each global land cover product by comparing our results to the reference data, i.e. deforestation drivers' classification by visual assessment. It gives us overall (e.g. overall accuracy) and per deforestation drivers summary metrics of land cover classification accuracy class (e.g. commission and omission error) at continental scale (see equation 2.1, 2.2 and 2.3). The structure of the confusion matrix and the calculation of the classification assessment are illustrated in figure 2.4.

Predicted Class \ Actual Class	A	B	C	D	Σ
A	n_{AA}	n_{AB}	n_{AC}	n_{AD}	n_{A+}
B	n_{BA}	n_{BB}	n_{BC}	n_{BD}	n_{B+}
C	n_{CA}	n_{CB}	n_{CC}	n_{CD}	n_{C+}
D	n_{DA}	n_{DB}	n_{DC}	n_{DD}	n_{D+}
Σ	n_{+A}	n_{+B}	n_{+C}	n_{+D}	n

$$Omission\ error = \left(1 - \left(\frac{n_{ii}}{n_{+i}}\right)\right) \times 100 \quad (2.1)$$

$$Commission\ error = \left(1 - \left(\frac{n_{ii}}{n_{i+}}\right)\right) \times 100 \quad (2.2)$$

$$Overall\ accuracy = \frac{\sum_{k=1}^{q} n_{kk}}{n} \times 100 \quad (2.3)$$

Figure 2.4: The confusion matrix and the measures of classification accuracy. Source: adapted from Foody, G. (2001)

2.2. Gross carbon emission estimates per deforestation driver

Estimates of carbon emissions from deforestation require information on both the area of forest loss over time and the changes in carbon stocks on land that is cleared. Both terms (area and changes in carbon stocks) can be represented on a gross or net basis. This thesis focused on the gross carbon emission estimates from deforestation only. In addition, we decided to focus our analysis in the South American continent where there is currently a more robust sample-based deforestation driver analysis than in Africa and in South-East Asia. Figure 2.5 gives a general overview of the different steps that were followed for the gross carbon estimates per driver between 1990-2000 and 2000-2005. More details on the different steps are given in the next sections. All developing steps were conducted with R (R Development Core Team, 2013) and supported by ArcGIS 10.1 and Google Earth for visualization.

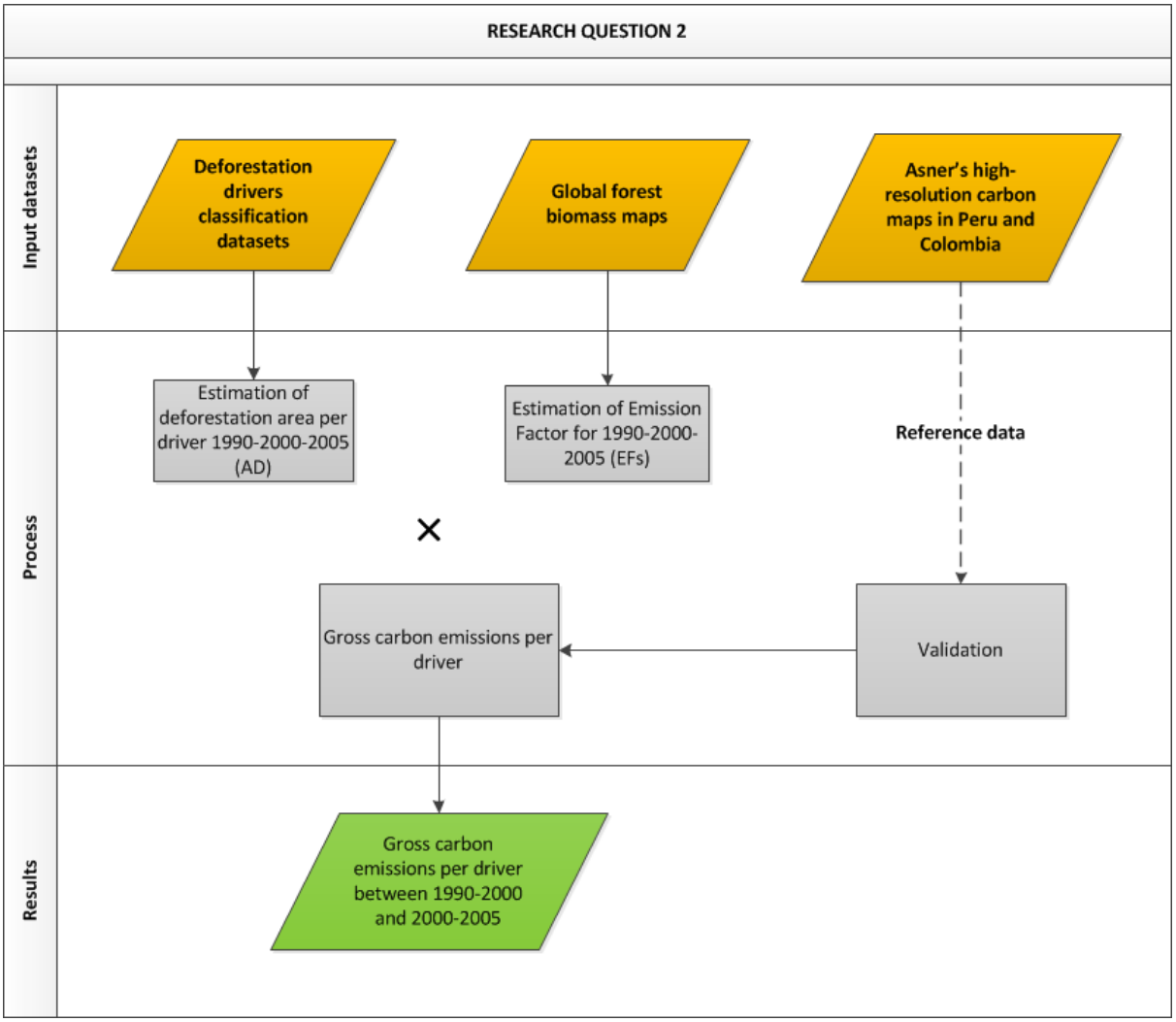

Figure 2.5: Flowchart of the method for gross carbon emissions per drivers between 1990-2000 and 2000-2005.

2.2.1. Data acquisition

In order to carry out the estimation of gross carbon emissions related to deforestation drivers, this study combined forest biomass maps and deforestation driver data. The changes in land use and the deforestation rate estimates were based on the previous analysis of the deforestation drivers by using the sample-based driver data (see sampling design in section

2.1.1). The estimates of forest carbon stocks were based on Yong forest biomass product (Yong *et al.*, 2014). This product is a fusion of the Saatchi forest biomass product (Saatchi *et al.*, 2011) available at the Jet Propulsion Laboratory, California Institute of Technology website (http://carbon.jpl.nasa.gov/data/dataMain.cfm) and the Baccini forest biomass product (Baccini *et al.*, 2012) available at the Woods Hole Research Centre website (http://www.whrc.org/mapping/pantropical/carbon_dataset.html). Both Baccini and Saatchi maps use spaceborne LiDAR data from the Geoscience Laser Altimeter System (GLAS) as samples of forest structure distributed across the tropics, but the two approaches use a different method to extend the isolated GLAS footprints to full-coverage AGB maps. Yong map at 1km resolution is based on a fusion method to increase the accuracy of regional biomass estimates by using higher-quality calibration data. In this fusion method, the biases in the source maps were first adjusted to correct for over- and underestimation by comparison with the calibration data. In addition, the FAO Ecozone Map (FAO, 2012) (figure 2.6) available at the FAO website (http://www.fao.org/geonetwork/srv/en/main.home) was combined with aboveground biomass map in order to estimate carbon emissions for the major tropical ecosystems (tropical rainforests, moist deciduous forests, dry forests, mountain ecosystems, shrubland, subtropical humid forests and steppe).

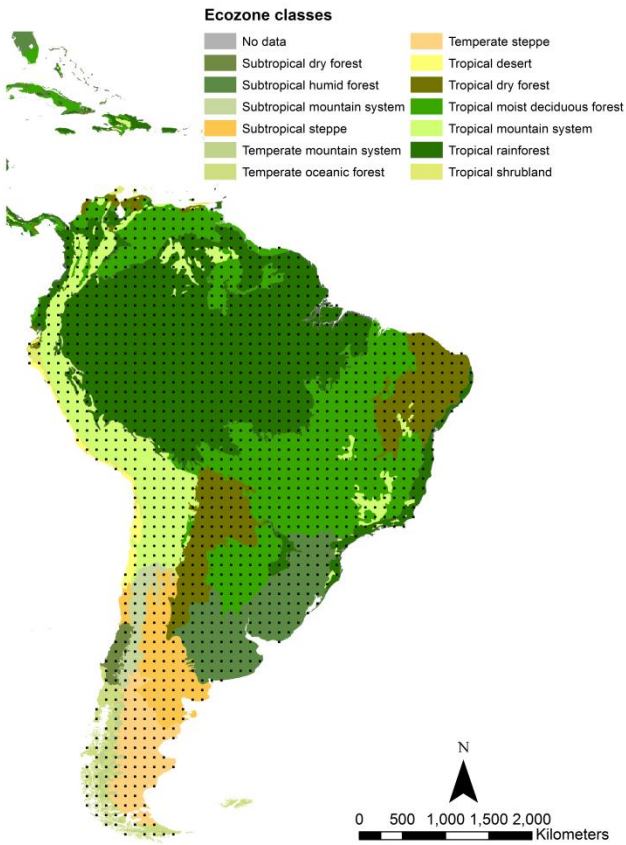

Figure 2.6: FAO Ecozone map in South America. The black squares represent our sample design. Source: FAO (2012)

2.2.2. Gross carbon emission estimates

This study followed the Guidelines for National GHG Inventories (IPCC, 2006) to quantify carbon emissions per driver. The methodological approach consists of combining information on the extent of human activities called activity data (AD) with coefficients that quantify emissions or removals per unit area called emission factors (EFs) (figure 2.7). We considered

only the areas that were classified as forest at the beginning of a defined time interval - either for the years of 1990 or 2000 time period - and then converted to non-forest by the end of the time interval.

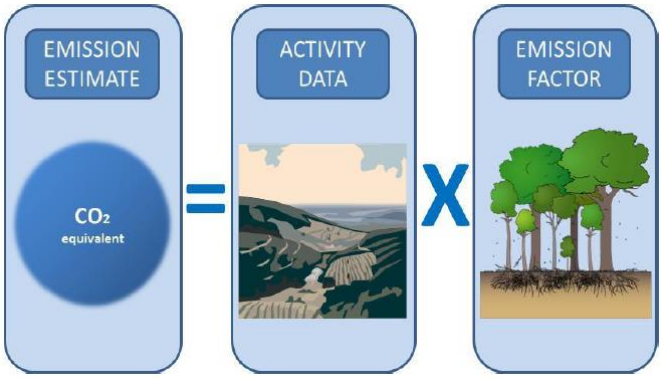

Figure 2.7: Methodological approach of the IPCC to calculate human-induced GHG emissions by sources and removals by sinks in forestland. Source: IPCC (2006).

The estimates of AD were determined by using the sample-based deforestation driver analysis carried out by the work of Veronique De Sy, whilst total forest biomass carbon stocks were estimated using Yong *et al.* (2014). In order to estimate the EFs, we assigned a biomass value before deforestation, called $biomass_{before}$, and a biomass value after deforestation, called $biomass_{after}$, to each deforested patches in order to estimate the biomass loss from deforestation. However, there is no data available to estimate the $biomass_{before}$ in a deforested patch because the temporal resolution of the forest biomass map is circa 2000. Therefore, we made the assumption that forest patches in the same ecozone than a deforested patch well-represent the $biomass_{before}$ value of the deforested patch. In addition, as the forest and deforested polygons included in our study usually contain fragmented land cover and are relatively small leading to a limited number of 1 km resolution pixels (Achard *et al.*, 2014), we considered for the driver classes (e.g. forest, agriculture, other land use, etc.) the average $biomass_{before}$ and $biomass_{after}$ values in each ecosystem. The biomass loss per driver was then estimated by subtracting the $biomass_{before}$ and $biomass_{after}$ values. Figure 2.8 summarizes the different steps followed for the biomass loss estimates.

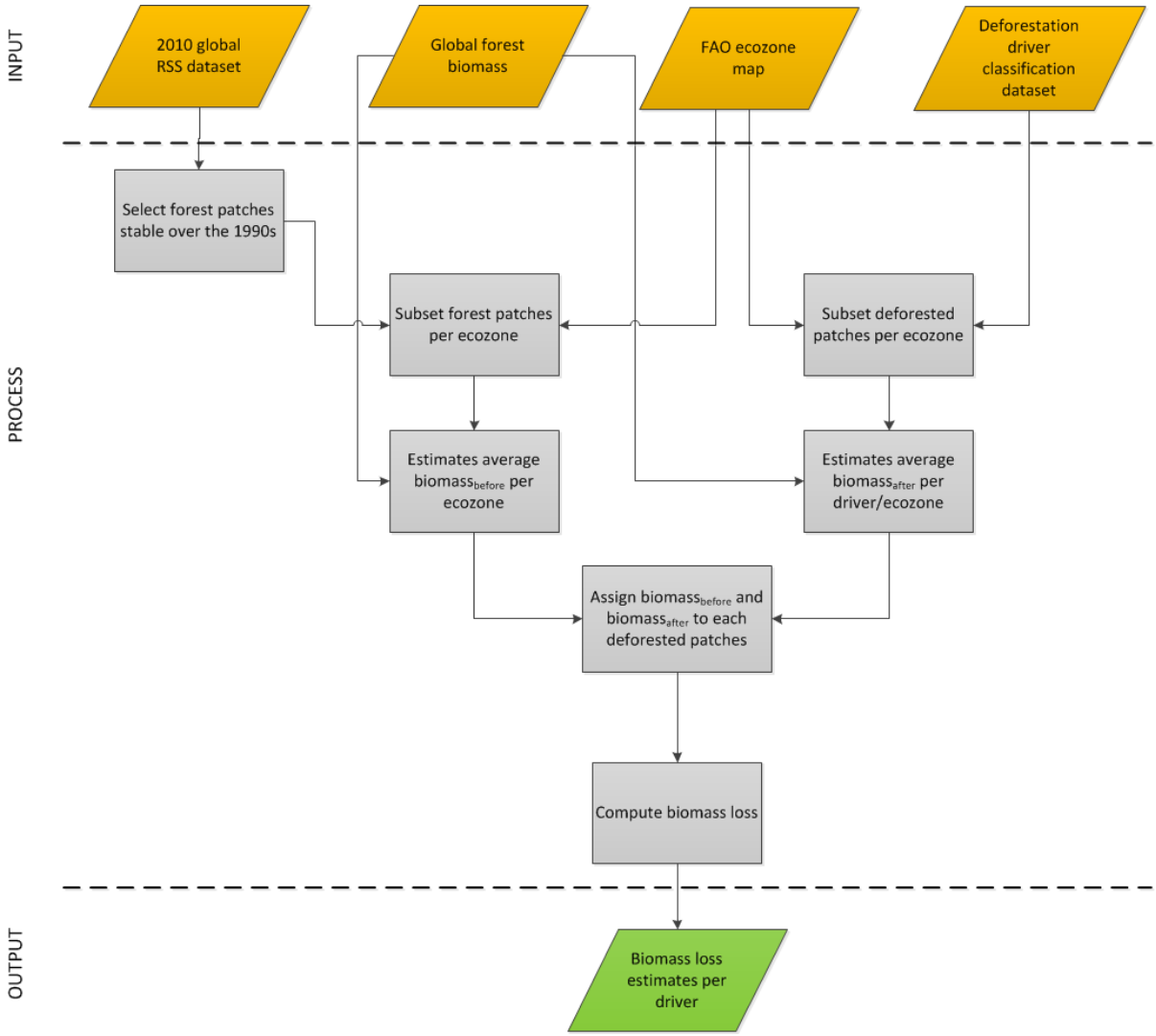

Figure 2.8: Flowchart of the biomass loss estimates per driver

Furthermore, Yong *et al.* (2014) only estimate the AGB and above-ground carbon portion. Therefore, we derived the total carbon estimates (above and below-ground) by using the equation 2.4 used by Saatchi *et al.* (2011):

$$Total\ Biomass = AGB + 0.489 \times AGB^{0.89} \quad (2.4)$$

where AGB is the aboveground biomass loss estimates.

In order to compute the EFs per driver, we estimated the total carbon as 49% of total biomass (Asner *et al.*, 2014; 2012). The same EF estimates were applied for the 2000-2005 time period. Finally, we estimated the carbon emissions from deforestation for the periods 1990-2000 and 2000-2005 as the product of net forest loss per driver and total forest biomass carbon stocks loss. Our method, therefore, assumed that all carbon in AGB is emitted immediately to the atmosphere at the time of clearing as we did not attempt to track the fate of all carbon pools through time.

The proportions of gross carbon emission per sample unit were then extrapolated to the continental level. To do so, several variables were calculated. First, we computed the area of land (*gla*) within the tile using equation 2.5:

$$gla = total - water - nodata \quad (2.5)$$

Where *total* is the total area in the tile, *water* and *nodata* are the areas of water and no data in the tile, respectively.

Then, we computed a latitude correction factor (*corrlat*) for each tile. This was done to avoid an increasing "weight" of samples in the high latitudes due to the curvature of the Earth (FAO, 2010).

$$\begin{gathered} if\ lat \leq 60°\ then\ corrlat = \cos(lat) \\ if\ lat \geq 60°\ then\ corrlat = 2 \times \cos(lat) \end{gathered} \quad (2.6)$$

These two variables allowed us to calculate the weight of the sample i (w_i) using the following equation:

$$w_i = \frac{gla_i \times corrlat_i}{\sum_i gla_i \times corrlat_i} \quad (2.7)$$

where *gla* is the area of land within a tile and *corrlat* is a latitude correction factor.

The next step was to annualize our carbon losses estimates (*paloss*). Equation 2.8 gives an example for the 1990-2000 time period:

$$paloss9000 = \frac{loss9000}{gla \times (jdate00 - jdate90)} \quad (2.8)$$

where *loss9000* is the carbon loss in 1990-2000 and *jdate00* and *jdate90* are the julian date of image acquisition for 1990 and 2000, respectively.

The samples 'average value of carbon losses at continental scale ($\overline{paloss9000}$ for the $1990-2000$ time period) and standard deviation (*std*) were then calculated using the following equations:

$$\overline{paloss9000} = \frac{\sum_{i \in S} W_i \times paloss9000}{\sum_{i \in S} W_i} \quad (2.9)$$

$$std = \sqrt{\frac{\sum_{i \in S} W_i \times (paloss9000 - \overline{paloss9000})^2}{\sum_{i \in S} W_i}} \quad (2.10)$$

where W_i is the weight of the sample i and *paloss9000* is the carbon loss of the sample i between 1990 and 2000.

Final values of annual carbon loss in forest area either during the 1990s and the 2000s at continental level (*total carbon loss*) were then obtained by multiplying the average of carbon losses ($\overline{paloss9000}$) and the standard deviation (*std*) by the area of the South American continent (*A*) provided by FAO (2010):

$$total\ carbon\ loss\ 9000 = \overline{paloss9000} \times A\ \pm 1.96\ \times \frac{std}{\sqrt{N}} \times A \quad (2.11)$$

where $\overline{paloss9000}$ is the average value of gross carbon emission, *std* is the standard deviation of gross carbon emission, *A* is the total areas of the South America continent and *N* is the total number of samples.

2.2.3. Method for validation

There are still few reference datasets available for validation of carbon emission estimates. However, we were able to validate the carbon emission estimates in two different countries: Colombia and Peru. As reference data, we used a high-resolution mapping of carbon stocks in the Colombian Amazon and in Peru developed by Asner *et al.* (2012) and Asner *et al.* (2014), respectively. These two maps were made by Airborne LiDAR technology and are available at the Canergie Air Observatory Website (https://codex.dge.carnegiescience.edu/groups/cao/maps). We used a linear regression to compare carbon emission estimates from Yong *et al.* (2014) forest biomass map and Asner *et al.* (2014; 2014) carbon stock maps. We therefore calculated the root mean squared error with respect to the 1:1 line to evaluate the deviation from the reference data.

Chapter 3. Assessment of global land cover maps for deforestation drivers analysis

3.1. Results

In this section, the results of the different global land cover products for deforestation drivers' detection for both Africa and South America will be described. For each land cover product, summary metrics of land cover classification accuracy such as omission error, commission error and overall accuracy will be presented. There are four driver' classes included in our assessment analysis: agriculture, infrastructure, other land use and water.

3.1.1. Assessment of global land cover products in Africa

Table 3.1 shows the area proportion of the four drivers from the three global land cover maps. Overall, agriculture and other land use driver classes have the highest area proportion while water and infrastructure make up a much smaller proportion of the driver classification. For both MODIS and CCI-LC datasets, agriculture is the most common driver while other land use constitutes the predominant driver in GLC-SHARE product.

Table 3.1: Area proportions in percentage per driver in the land cover maps in Africa.

	MODIS		GLC-SHARE		CCI-LC	
	2000	**2005**	**2000**	**2005**	**2000**	**2005**
Agriculture	72.0	80.1	34.6	25.6	89.9	90.4
Infrastructure	NA	0.1	NA	0.1	0.3	NA
Other land use	27.7	19.8	64.9	74.1	9.7	9.4
Water	0.3	NA	0.6	0.2	<0.1	0.2

Table 3.2 lists the results of the accuracy assessment for each land cover type in both the baseline year 2000 and 2005 using MODIS datasets. The table indicates that agriculture driver class has the lowest omission errors (or the highest producer accuracy) for both 2000 and 2005 with percentage values of 20.5% and 16.1%, respectively, while infrastructure (100.0% and 97.4% for 2000 and 2005, respectively), other land use (55.1% and 74.9% for 2000 and 2005, respectively), are somewhat higher (table 3.2). Agriculture has the lowest commission error (or the highest user accuracy) in 2000 (22.2%) while infrastructure has the lowest commission error in 2005 (0.0%). However, the latter result has to be interpreted carefully as the total area of infrastructure represents only 0.1% of the total area. A high commission error, i.e. 54.3% for other land use class in 2005, indicates that a small number of areas that are not other land use are committed to this class. The overall accuracies of the MODIS datasets in our study are 68.7% and 59.7% for 2000 and 2005, respectively.

Table 3.2: Confusion matrix for MODIS land cover map in Africa.

	Omission error (%)		Commission error (%)		Overall accuracy (%)	
	2000	**2005**	**2000**	**2005**	**2000**	**2005**
Agriculture	20.5	16.1	22.2	36.8	**68.7**	**59.7**
Infrastructure	100.0	97.4	NA	0.00		
Other land use	55.1	74.9	54.0	54.3		
Water	100.0	100.0	100.0	NA		

Table 3.3. illustrated the results for GLC-SHARE dataset. The table shows that other land use class has the lowest omission errors for both 2000 and 2005 of 19.9% and 15.3%, respectively, while agriculture (54.9%, 67.9% for 2000 and 2005, respectively), infrastructure

(100.0% and 95.9% for 2000 and 2005, respectively) and water (87.3% and 79.2% for 2000 and 2005, respectively) classes show higher omission errors. However, agriculture has the lowest commission error in 2000 (25.6%) while infrastructure has the lowest commission error in 2005 (21.5%). Again, the latest result has to be analysed carefully as the area of infrastructure represents only 0.1% of the total area. It can be observed that the overall accuracies of GLG-SHARE datasets for the deforestation driver classification are around 60.00% and around 50.00% for 2000 and 2005, respectively.

Table 3.3: Confusion matrix for GLC-SHARE land cover map in Africa.

	Omission error (%)		Commission error (%)		Overall accuracy (%)	
	2000	**2005**	**2000**	**2005**	**2000**	**2005**
Agriculture	54.9	67.9	25.6	24.2	**58.8**	**51.9**
Infrastructure	100.0	95.9	NA	21.5		
Other land use	19.9	15.3	49.3	56.1		
Water	87.3	79.2	85.3	84.3		

Table 3.4 demonstrates that agriculture driver has the lowest omission errors for both 2000 and 2005 with error values of 6.4% and 6.0%, respectively with CCI-LC products. Infrastructure (100.0% for both 2000 and 2005), other land use (85.7% and 85.5% for 2000 and 2005, respectively) and water (20.9% and 19.3% for 2000 and 2005, respectively) show higher omission errors. However, water has the lowest commission error in 2000 (9.7%) while infrastructure has the lowest commission error in 2005 (36.9%). The overall accuracies of CCI land cover maps for our study are 57.9% and 60.5% for 2000 and 2005, respectively.

Table 3.4: Confusion matrix for CCI land cover map in Africa.

	Omission error (%)		Commission error (%)		Overall accuracy (%)	
	2000	**2005**	**2000**	**2005**	**2000**	**2005**
Agriculture	**6.4**	**6.0**	42.7	39.8	**57.9**	**60.5**
Infrastructure	100.0	100.0	100.0	NA		
Other land use	85.7	85.5	36.5	36.9		
Water	20.9	19.3	9.7	38.6		

Furthermore, it is also relevant to see how the omitted and committed errors are allocated amongst the other driver classes. Figure 3.1 emphasizes that most of the commission error results from confusion with both the agriculture and other land use classes. Figure 3.1a and 3.1b show the repartition of the committed and omitted deforested areas per driver for CCI2000 and CCI2005 products, respectively. Figure 3.1a and figure 3.1b show that most of the omitted and the committed areas of agriculture are allocated in other land use class for both 2000 and 2005. In addition, the misclassified and omitted areas of the other land use class are related to agriculture class. Finally, figure 3.1a shows that the omission and commission errors for both infrastructure and water classes are distributed amongst the agriculture driver class (e.g. 99.1% and 0.0% of omission error and commission error, respectively for infrastructure) and other land use class (e.g. 0.9% and 100.0% of omission error and commission error, respectively for infrastructure). Figure 3.1b shows that a similar tendency occurs in 2005.

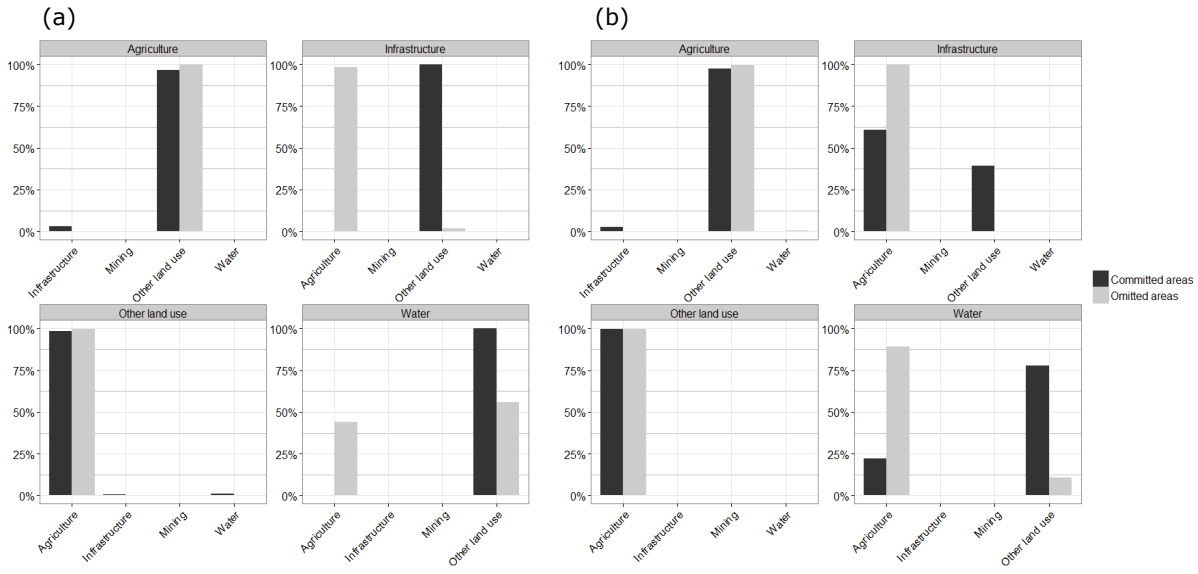

Figure 3.1: Distribution of the committed and omitted deforested areas per driver for CCI2000 (figure 3.1a) and CCI2005 (figure 3.1b) land cover maps in Africa.

3.1.2. Assessment of global land cover products in South America

Table 3.5 shows the area proportion of the four drivers from the three global land cover maps in South America. Overall, we found similar results than in Africa. Agriculture and other land use driver classes comprise the majority of the drivers' area proportion in the three products with agriculture being the most common class for the three datasets. Again, water and infrastructure make up a smaller proportions.

Table 3.5: Area proportions in percentage per driver in the land cover maps in South America.

	MODIS		GLC-SHARE		CCI-LC	
	2000	**2005**	**2000**	**2005**	**2000**	**2005**
Agriculture	75.2	65.3	71.2	59	93.4	88.2
Infrastructure	0.1	2	NA	1.0	0.2	1.6
Other land use	24.3	32.2	27.6	37.1	5.7	8.1
Water	0.4	0.5	1.2	2.9	0.7	2.1

The confusion matrix for MODIS products depicts that agriculture driver has the lowest omission errors for both 2000 and 2005: 23.0% and 29.7%, respectively. Infrastructure (70.1% and 51.1% for 2000 and 2005, respectively), other land use (66.9% and 42.6% for 2000 and 2005, respectively), have somewhat higher omission and commission errors (table 3.6). Water has the lowest commission errors in 2000 (0.0%) and in 2005 (0.0%). However, this result has to be interpreted carefully as the area of water comprises only 0.1% of the total area. The overall accuracies of MODIS dataset in South America are 72.9% and 67.1% for 2000 and 2005, respectively.

Table 3.6: Confusion matrix for MODIS land cover map in South America.

	Omission error (%)		Commission error (%)		Overall accuracy (%)	
	2000	**2005**	**2000**	**2005**	**2000**	**2005**
Agriculture	23.0	29.7	5.5	6.9	**72.9**	**67.1**
Infrastructure	70.1	51.1	43.4	4.8		
Other land use	66.9	42.6	93.5	88.1		
Water	95.7	80.8	0.0	0.0		

Table 3.7 shows that agriculture (25.7%) has the lowest omission errors for 2000 while water (15.4%) has the lowest omission error in 2005 with the GLC-SHARE dataset. Agriculture has the lowest commission error for both 2000 (4.1%) and 2005 (5.1%). The overall accuracies of the GLG-SHARE datasets in South America for the deforestation driver classification are 72.6% and 88.4% for 2000 and 2005, respectively.

Table 3.7: Confusion matrix for GLC-SHARE land cover map South America.

	Omission error (%)		Commission error (%)		Overall accuracy (%)	
	2000	**2005**	**2000**	**2005**	**2000**	**2005**
Agriculture	25.7	36.4	4.1	5.1	**72.6**	**88.4**
Infrastructure	100.0	65.6	NA	5.2		
Other land use	42.6	39.3	87.3	88.9		
Water	37.9	15.4	31.2	27.4		

CCI land cover maps shows better results in South America than the previous two land cover products (table 3.8). The confusion matrix for CCI land cover product illustrates that agriculture driver has the lowest omission and commission errors for both 2000 and 2005 with percentage values of 4.8%, 7.1%, 5.1% and 5.1%, respectively. Infrastructure, other land use and water show higher omission and commission errors (table 3.8). The overall accuracies of CCI land cover maps in South America are 90.2% and 88.4% for 2000 and 2005, respectively.

Table 3.8: Confusion matrix for CCI land cover map in South America.

	Omission error (%)		Commission error (%)		Overall accuracy (%)	
	2000	**2005**	**2000**	**2005**	**2000**	**2005**
Agriculture	**4.8**	**7.1**	**5.1**	**5.1**	**90.2**	**88.4**
Infrastructure	83.9	34.1	33.8	12.0		
Other land use	83.9	73.6	86.1	81.5		
Water	40.8	18.3	5.9	18.5		

Figure 3.2a and 3.2b depicts the repartition of the committed and omitted deforested areas per driver for CCI2000 and CCI2005 products, respectively. As already shown in Africa (see figure 3.1a and figure 3.1b), most of the omitted and the committed areas of agriculture are allocated in other land use driver class for both 2000 and 2005. The commission and omission errors of other land use class are due to agriculture driver class. Similar to Africa, figure 3.2a and 3.2b show that the omission and commission errors for both infrastructure and water classes are distributed amongst agriculture driver class (e.g. 92.0% and 65.0% of omission error and commission error, respectively for infrastructure in 2000) and other land use class (e.g. 8.0% and 35.0% of omission error and commission error, respectively for infrastructure in 2000).

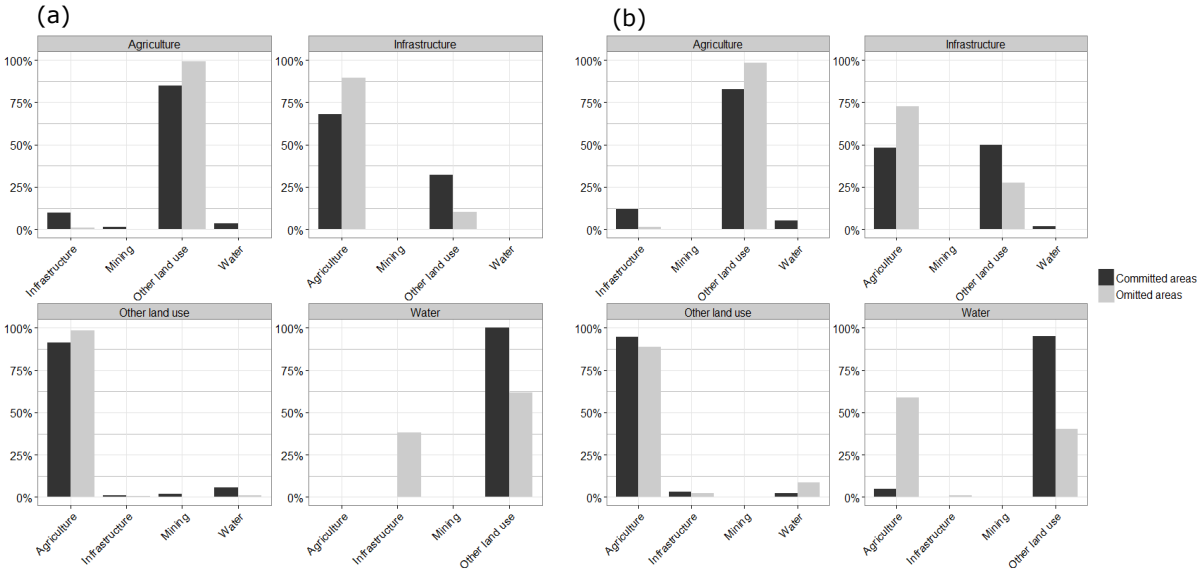

Figure 3.2: Distribution of the committed and omitted deforested areas per driver for CCI2000 (figure 3.2a) and CCI2005 (figure 3.2b) land cover maps in South America.

3.2. Discussion

3.2.1. Suitability of global land cover maps in Africa

In Africa, the deforestation drivers' classification is estimated to be rather uncertain in all datasets (see overall accuracies estimates of the three products). In general, water and infrastructure classes show the lowest overall mapping accuracies. However, water and infrastructure have an area proportion rather low compared to agriculture and other land use classes, therefore this findings have to be interpreted carefully. Other land use class also has low overall mapping accuracies, expect for GLC-SHARE product where this class has the highest producer accuracy. In particular, CCI-LC maps indicate the lowest producer and user accuracies for this class. Moreover, it seems that GLC-SHARE map shows lower omission error and higher commission errors for other land use class. For all the datasets, a lot of confusion exists between this class and agriculture (see figure 3.1 for CCI-LC products). A similar pattern exists for water and infrastructure with major confusion between these classes and both agriculture and other land use classes. Furthermore, MODIS500 and CCI-LC products were relatively proficient for the agriculture class in our study. Nevertheless, the commission error for this class is relatively high in CCI-LC maps (see table 3.4) with a lot of confusion with other land use class.

Therefore, our study highlights a general inability of the global land cover mapping approaches to clearly discriminate deforestation drivers in Africa. Confusion in the deforestation drivers' classes could be explained by a wrong classification of this class in the reference dataset but also by scaling effects between validation dataset (visual assessment using Landsat datasets) and the global land cover maps. Differentiating these deforestation drivers' classes is difficult with coarse resolution spectral-temporal data alone in the African continent. However, one could think about using CCI-LC maps in order to classify the agriculture class in Africa. The high producer's accuracy for this class using CCI-LC maps indicates an accurate mapping of all areas that actually represent this class on the ground. The main limitation of this suggestion is that agriculture class shows a low user accuracy,

therefore, users will likely overmap this class while using CCI-LC datasets (Herold *et al.*, 2008) for the analysis of deforestation drivers in Africa.

3.2.2. Suitability of global land cover maps in South America

Overall, our study shows better results on the capacity of global land cover maps for the analysis of deforestation drivers in South America than in Africa for the three datasets. However, the overall accuracy of these datasets is variable and only CCI-LC maps 'overall accuracies meet the nominal standard of 85% recommended by Anderson *et al.* (1976). Other land use class is estimated to be rather uncertain in all datasets and is mainly confused with agriculture class. Like in Africa, CCI-LC maps indicate the lowest producer and user accuracies for agriculture class. In addition, water and infrastructure show relative high omission and commission errors in all the datasets. However, water class demonstrates low commission error in the CCI2000 land cover map while infrastructure class has low commission errors in both MODIS2005 and GLC-SHARE products. The bottom line is that these two classes with high omission errors and low commission errors are under-mapped in our analysis. As shown in figure 3.2, most of the errors for these two classes result from confusion with agriculture and other land use classes. The accuracy of the agriculture classifications in our study were relatively high, probably because regionally abundant land cover classifications typically generate higher accuracy ratings (Wickham *et al.*, 2010).

In summary, our study demonstrates again that the coarse resolution of the global land cover maps is a limitation for deforestation drivers' classification. Only CCI-LC maps seem to have potential to analyse the deforestation drivers' classification, in particular for agriculture driver class which presents high overall mapping accuracies. Unlike in Africa, this class does not have a high commission error, therefore, one will not face overmapping issues for agriculture driver classification. In addition, some areas have been classified as other land use by the interpreter in the reference data, although they could have been classified as agriculture. Indeed, in some situations, by using a visual assessment approach, the interpreter was not capable of determining whether one area should be included in other land use class or in agriculture class instead. Therefore, CCI-LC maps could be also used in order to check whether one area has been correctly classified as other land use or should be, in fact, labelled as agriculture class.

Chapter 4. Gross carbon emission estimates per deforestation driver

4.1. Results

In this section, the results of the gross carbon emissions analysis per driver will be described. First, we will present the estimation of the biomass and EFs in each ecosystem. Second, the results of the total gross emissions per driver at continental level will be presented. Then, the changes overtime of carbon emissions driven by pasture expansion and crop agriculture will be described. Finally, the validation of our method will be presented.

4.1.1. Estimation of biomass and carbon losses in South America

Figure 4.1 shows the biomass estimates from the Yong forest biomass map for different land uses (e.g. forest, crop agriculture, mixed agriculture, tree crops, pasture, other land use, mining, water and infrastructure) in each ecosystem encountered in South America. However, one can see that not all the drivers are represented in the different ecosystems. For instance, in subtropical steppe ecozone, there are only forest, other land use and pasture land uses represented in our sample design. In addition, we decided to assign biomass values equal to zero for both water and infrastructure assuming that the AGB is null in these two land uses. We made this assumption because water and infrastructure patches are very small compared to the pixel size of the forest biomass map. Therefore, their biomass values are likely overestimated as they are most of the time surrounding by forest patches.

Overall, figure 4.1 depicts that forest land use has the highest biomass values in all the ecozones, except for the sub-tropical steppe ecozone (figure 4.1b). In addition, mixed agriculture class shows high biomass values compare to the other classes in most of the ecozones. Agriculture and pasture classes have, in general, the lowest biomass values, if one does not consider water and infrastructure classes. It is also interesting to see that tree crops class show both high biomass values (e.g. tropical mountain system ecozone) and low biomass values (e.g. tropical rainforest) compared to the other driver classes. Other land use class shows relatively high biomass values in the different ecozones. Figure 4.1 also demonstrates that there is high variability of the biomass values within most of the different land uses classes in each ecozone.

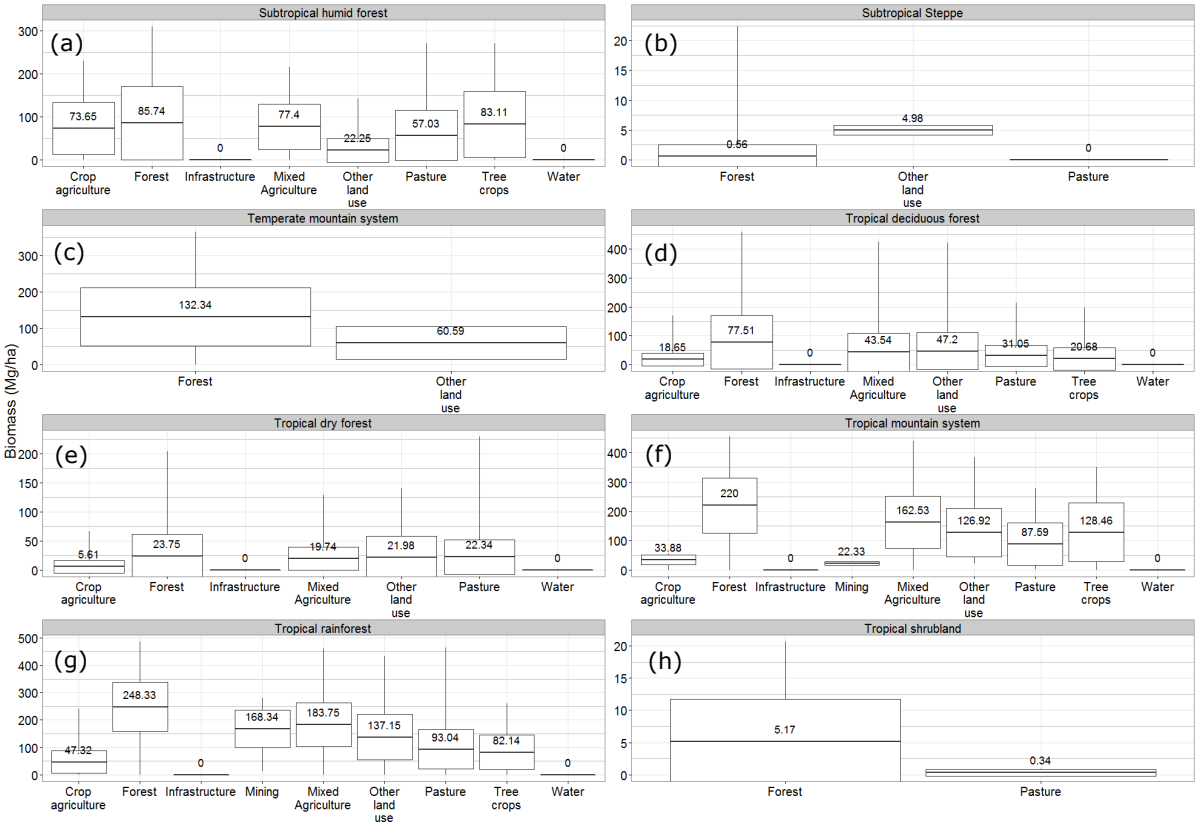

Figure 4.1: Average biomass estimates for land uses in subtropical humid forest (figure 4.1a), subtropical steppe (figure 4.1b), temperate mountain system (figure 4.1c), tropical deciduous forest (figure 4.1d), tropical dry forest (figure 4.1e), tropical mountain system (figure 4.1f), tropical rainforest (figure 4.1g) and tropical shrubland (figure 4.1h) ecozones.

Figure 4.2 illustrates the EF estimates per deforestation driver in each ecosystem. As described in the section 2.2.2, the EFs have been estimated by subtracting an average forest biomass value to the $biomass_{after}$ in a deforested patch at ecozone level. The biomass loss estimates were then converted into carbon loss by assuming that 49% of the biomass is made of carbon. If one does not consider water and infrastructure, crop agriculture shows, in general, the highest EF estimates followed by pasture. In tropical deciduous forest (figure 4.2b) and tropical dry forest (figure 4.2c), there is no significant differences of EF estimates between the classes. Conversely, there are significant differences between classes in tropical rainforest and tropical mountain systems ecozones. One can also see that in subtropical steppe ecozone, the average EF value of other land use class is negative (figure 4.2e). Further in our analysis, we considered this negative value as an outlier and replace it by a value of zero.

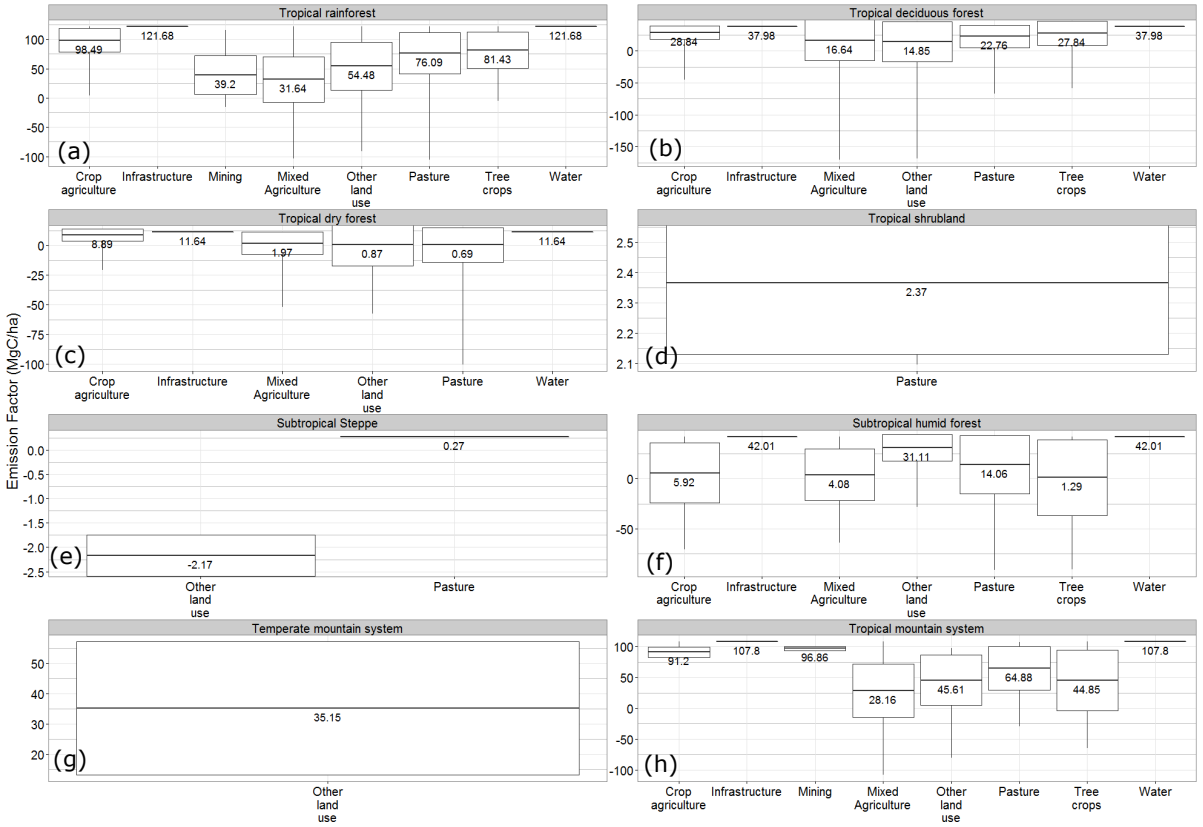

Figure 4.2: Average EF estimates per driver in tropical rainforest (figure 4.2a), tropical deciduous forest (figure 4.2b), tropical dry forest (figure 4.2c), tropical shrubland (figure 4.2d), subtropical steppe (figure 4.2e), subtropical humid forest (figure 4.2f), temperate mountain system (figure 4.2g), and tropical mountain system (figure 4.2h) ecozones.

4.1.2. Carbon emissions estimates per driver in South America

Figure 4.3 illustrates the annual gross emissions per driver in South America for 1990-2000 and 2000-2005 time periods with both absolute and percentage values. At continental scale, our estimates of annual carbon loss are 195 ±4.2 MtC.yr^{-1} and 246±4.9 MtC.yr^{-1} for the 1990s and the 2000s, respectively, thus showing significant difference for the two periods. Figure 4.3a also shows that agriculture (174.5 MtC.yr^{-1} and 227.2 MtC.yr^{-1} for 1990-2000 and 2000-2005, respectively) contribute the most to annual gross emissions followed by other land use (11.2 MtC.yr^{-1} and 11.1 MtC.yr^{-1}), water (7.6 MtC.yr^{-1} and 5.8 MtC.yr^{-1}), infrastructure (2.1 MtC.yr^{-1} and 1.8 MtC.yr^{-1}), and mining (1.4e^{-2} MtC.yr^{-1} and 0.9e^{-3} MtC.yr^{-1}). Within the agriculture class, pasture (149.2 MtC.yr^{-1} and 180.2 MtC.yr^{-1} for 1990-2000 and 2000-2005, respectively) has the highest annual gross emissions followed by crop agriculture (18.6 MtC.yr^{-1} and 39.1 MtC.yr^{-1}), mixed agriculture (5.2 MtC.yr^{-1} and 6.7 MtC.yr^{-1}), and tree crops (1.4 MtC.yr^{-1} and 1.2. MtC.yr^{-1}). Furthermore, figure 4.3b depicts that there are no significant changes within a driver class in terms of percentage of the total annual emissions for the two periods.

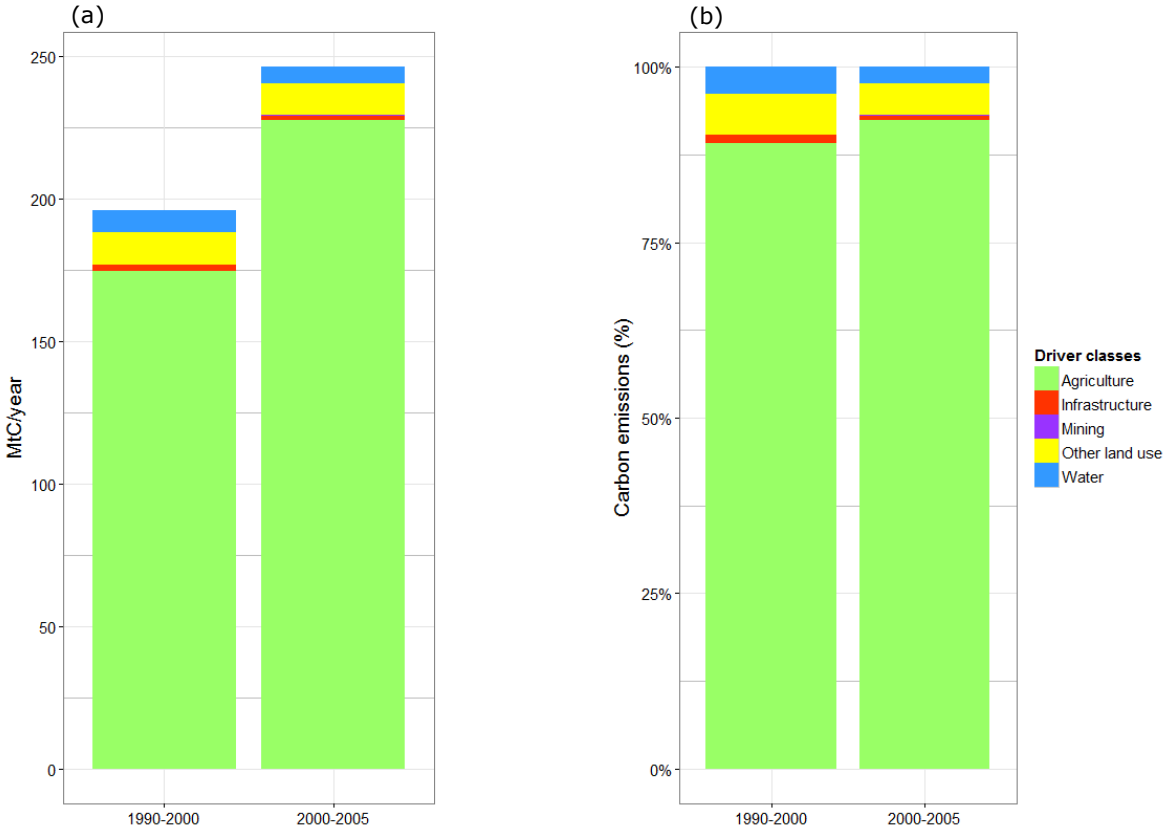

Figure 4.3: Absolute (figure 4.3a) and percentage (figure 4.3b) carbon emission values per driver for 1990-2000 and 2000-2005 in South America.

Our study highlights spatial and temporal patterns of carbon losses resulting from forest to non-forest (figure 4.4). The main area of carbon loss in both periods is in the so called 'arc of deforestation' of the Brazilian Amazon (red dashed line/circle in figure 4.4a), particularly in the Mato-Grosso and NE Brazil-Caatinga. In this specific area, carbon losses are mainly driven by pasture expansion with some patches of crop agriculture as well as other land use driver in smaller proportions. In addition, one can point out a hot-spot of carbon emissions in the area of the Colombian Amazon (black dashed circle in figure 4.4a). Our study also shows that there are high carbon emissions in the region of Santa-Cruz, Bolivia, mainly driven by crop agriculture, other land use and water (dark blue dashed ellipse in figure 4.4a). The study also shows the allocation of the annual gross emissions amongst the different ecozones in South America (figure 4.4b). Our results show that most of the carbon losses from deforestation occurred in tropical rainforest ecosystem (158 MtC.year^{-1} and 209 MtC.year^{-1} for the 1990s and the 2000s, respectively). This ecozone comprises around 80% of the annual total carbon losses at continental scale for the two time periods. Tropical deciduous forest ecozone (15.3% and 11.5% for 1990-2000 and 2000-2005, respectively) comprises the second largest annual gross carbon emissions followed by tropical dry forest (1.6% and 1.7% for 1990-2000 and 2000-2005, respectively). The other ecozones (e.g. subtropical humid forest, tropical shrubland, tropical/temperate mountain system, and subtropical steppe) comprise only a very small proportion of the annual carbon losses in South America.

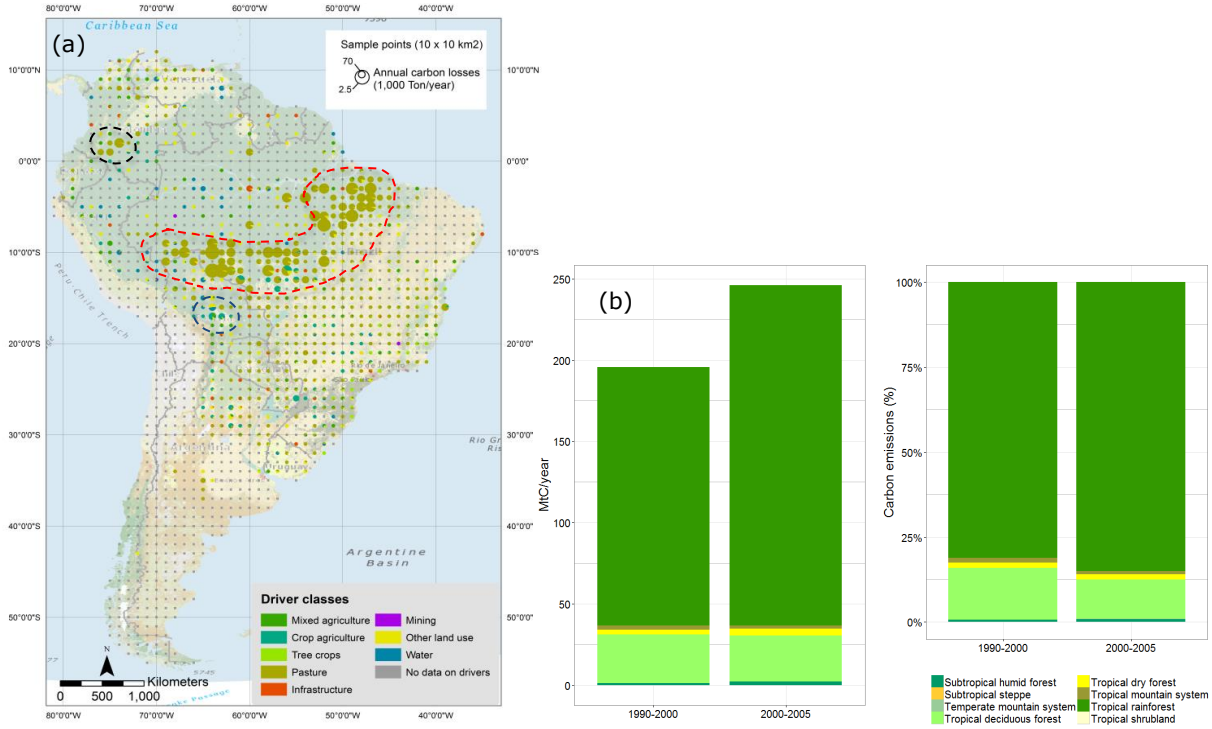

Figure 4.4: Spatial pattern of carbon losses per driver for the 1990-2005 time period (figure 4.4a) and the proportions carbon emission per ecosystem (figure 4.4b) in South America.

Our study also analyses the distribution of each driver amongst the different ecozones. Figure 4.5 shows all deforestation drivers mainly occur in the tropical rainforest ecozone. In addition, one can see that there are some changes between the two time periods. For instance, while around 60% of the annual carbon emissions from crop agriculture expansion occurred in tropical rainforest during the 1990s, around 80% took place in the same ecoregion during the 2000s. We found a similar tendency for mining class. Finally, figure 4.5 depicts that some drivers are limited to only two or three ecozones (e.g. crop agriculture, pasture and mining), while the other driver classes are ecologically more widespread.

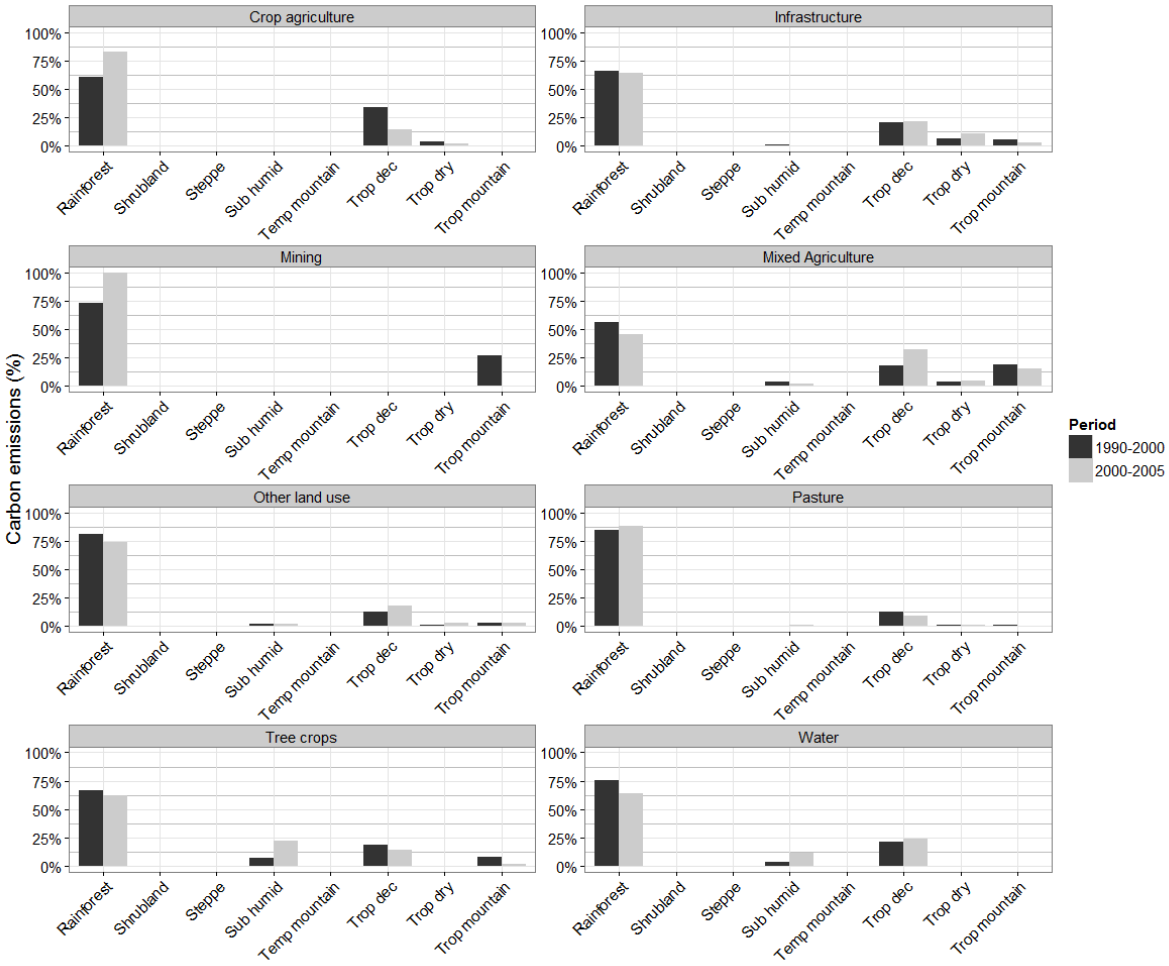

Figure 4.5: Proportions carbon emission per driver in the different ecozones for 1990-2000 and 2000-2005 in South America.

Figure 4.6 shows the changing of carbon losses driven by both pasture expansion and crop agriculture between the 1990s and the 2000s. The red pies show an increase of carbon emissions between the two periods while the green pies show a decrease in carbon emissions. Figure 4.6a shows clearly that new deforestation hot-spots related to pasture expansion took place deeper in the amazon rainforest in the 2000s than in the 1990s. Figure 4.6b also depicts new hotspots of carbon emissions from crop agriculture expansion to a lesser extent. However, crop agriculture expansion's new hotspots occurred mainly at the amazon forest 'frontier and anthropogenic activities related to crop agriculture have not progressed in the heart of the amazon rainforest as much as pasture.

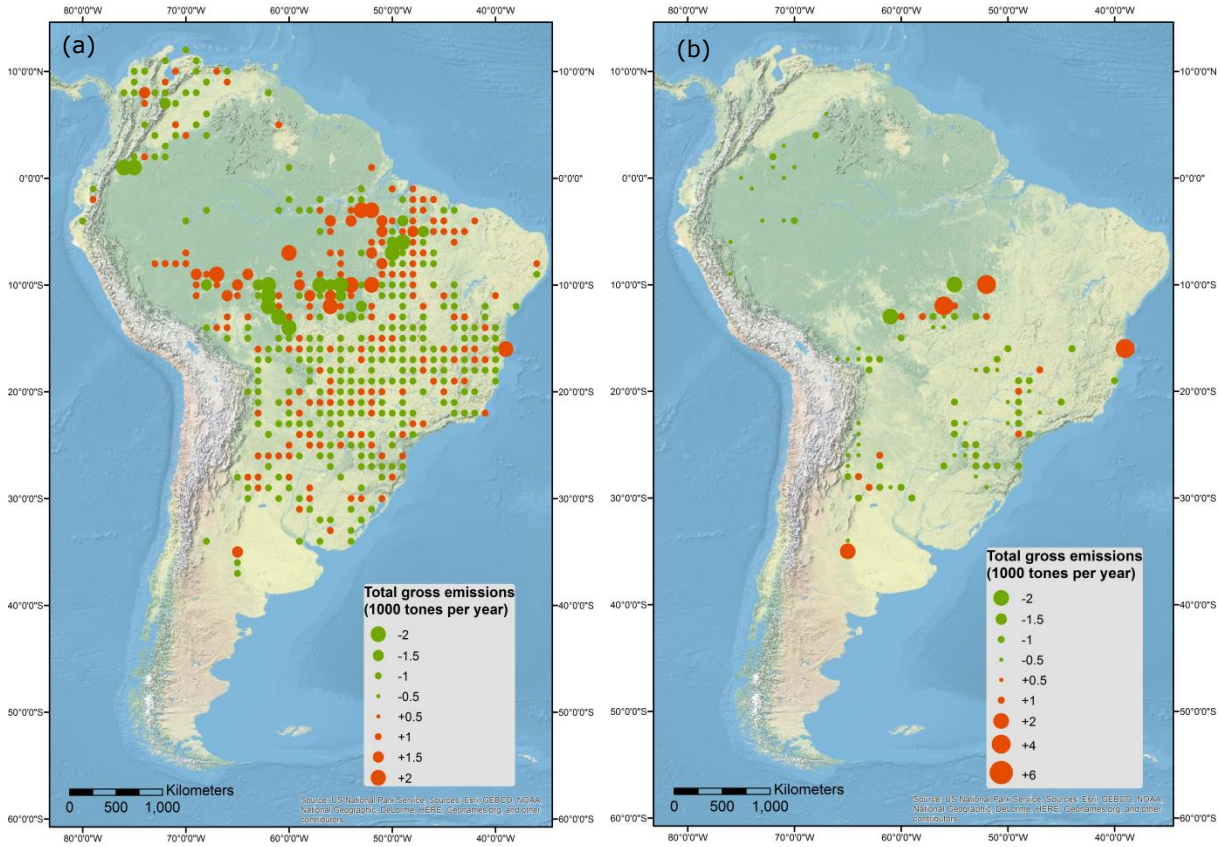

Figure 4.6: Changing carbon emissions driven by pasture expansion (figure 4.6a) and crop agriculture (figure 4.6b) between 1990 -2000 and 2000 -2005 time period

4.1.3. Validation method

The comparison of forest biomass map derived EFs values against Asner carbon stocks maps EFs values is shown in figure 4.7. The RMSE with respect to the 1:1 line is 38.51 MgC/ha for the EF estimates. Our method does not show a linear fit with the reference carbon stock data for the EF estimates with a slope of 0.96 and a R-squared of 0.266. In addition, figure 4.7 shows that water and mixed agriculture driver classes tend to be overestimated using the Yong global forest biomass map while other land use, mining, crop agriculture and pasture are underestimated. We assess the potential bias of our results by comparing EF estimates derived from our study to EF estimates derived from the reference datasets. The average relative difference is a -20% lower EF estimate from our study compared to the reference dataset. The highest bias occurred in the Colombian's tropical rainforest for the 'other land use' driver where the relative difference is -92.3% whilst the Peruvian tropical rainforest has the lowest bias (-6.1%) for the same driver.

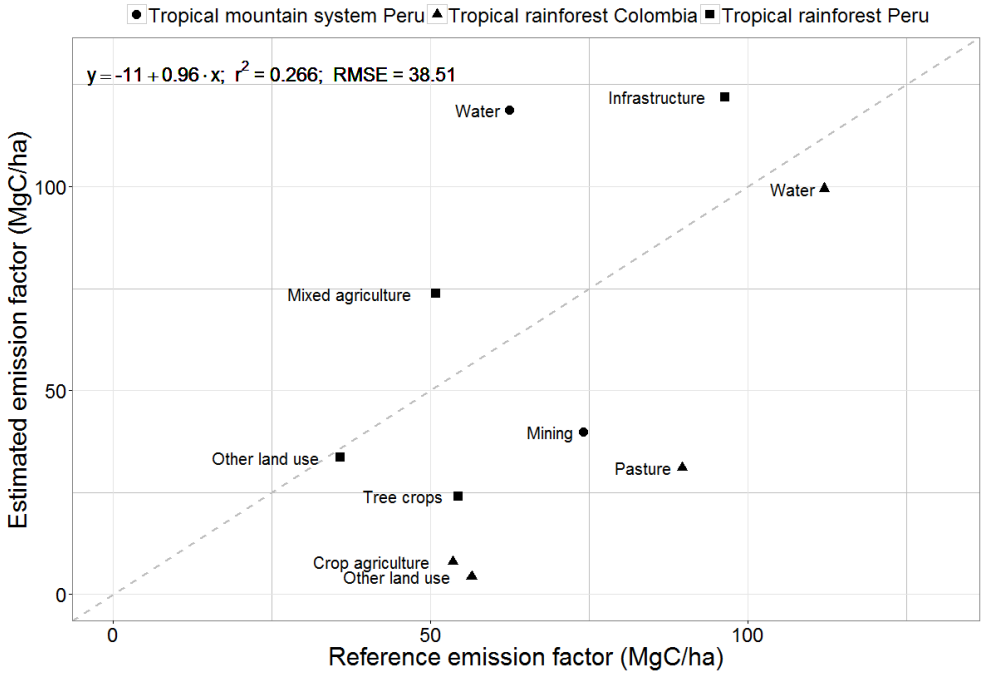

Figure 4.7: Comparison of forest biomass maps derived emission factor values with Asner carbon stocks map emission factor values.

4.2. Discussion

In this section, we will discuss the results obtained during the carbon emissions analysis in South America. First, we will compare our estimates of forest biomass with the IPCC AFOLU guidelines (2006). Then, we will liken our findings to the estimates of both EFs and annual gross carbon losses with other studies. Finally, we will analyse the spatial patterns of carbon losses in the South American continent.

4.2.1. Comparison forest biomass estimates with other studies

Our estimates of forest biomass for the year 2000 in tropical rainforest, tropical moist deciduous forest, tropical dry forest, tropical shrubland, tropical mountain systems, subtropical humid forest, subtropical steppe and the temperate mountain systems ecozones are 250 $Mg.ha^{-1}$, 80 $Mg.ha^{-1}$, 25 $Mg.ha^{-1}$, 5 $Mg.ha^{-1}$, 220 $Mg.ha^{-1}$, 85 $Mg.ha^{-1}$, 1 $Mg.ha^{-1}$ and 132 $Mg.ha^{-1}$, respectively. Table 4.1 depicts that our estimates for tropical rainforest, tropical moist deciduous forest, tropical dry forest, tropical shrubland, tropical mountain systems, subtropical humid forest, and subtropical steppe ecozones are 20%, 175%, 740%, 1500%, 4.5%, 160%, 7900% lower than the IPCC AFOLU guidelines (2006) estimates, respectively. Conversely, our estimate of forest biomass in temperate mountain system ecozone is 3.7% higher than the IPPC estimates. The FAO (2010) forest biomass estimate is 245 Mg/ha. However, this study does not give an estimate of forest biomass per ecozone but rather gives an average value from all the ecozones.

Table 4.1: Forest Biomass estimates in different ecozones from our study and the IPCC AFOLU Guidelines (2006) in South America.

Domain	Ecological zone	Aboveground Biomass (Mg.ha^{-1}) from IPCC (2006)	Aboveground Biomass (Mg.ha^{-1}) from this study	Area included per tile (km^2) from this study
Tropical	Tropical rainforest	300	250	18,000
	Tropical moist deciduous forest	220	80	4,600
	Tropical dry forest	*210*	*25*	*3,100*
	Tropical shrubland	*80*	*5*	*14*
	Tropical mountain systems	230	220	2,500
Subtropical	Subtropical humid forest	220	85	760
	Subtropical steppe	*80*	*1*	*240*
Temperate	Temperate mountain systems	130	135	380

The discrepancies between the IPCC estimates and our study can be explained by the spatial resolution of the Yong biomass map (1 km resolution) and the size of the FRA2010 polygons. Figure 4.8a shows some FRA2010 polygons overlapping the Yong biomass map. It is clear that some pixels comprise both forest and deforested polygons (red dashed circle in figure 4.8a). Therefore, when forest and non-forest land uses are mixed within one pixel, this would very likely lead to both an underestimation of the forest biomass and an overestimation of the non-forest land uses biomass. This is confirmed by the high variability of biomass estimates shown in figure 4.1. High resolution carbon maps, such as Asner's maps used for the validation of our results, do not seem to have this issue in which there is no forest and non-forest polygons mixed in one pixel (figure 4.8b).

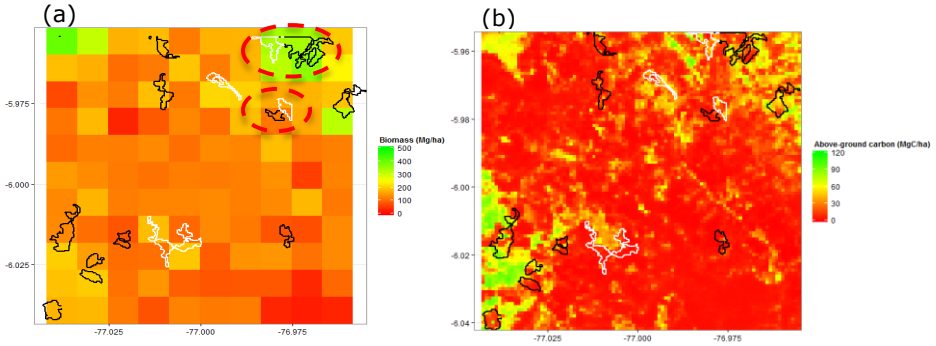

Figure 4.8: Representation of forest (in black) and deforested (in white) polygons on the biomass map for Yong map (figure 4.8a) and Asner map (figure 4.8b).

Nevertheless, this assumption cannot completely explain the very high variations between our study and the IPCC estimates in ecozones such as tropical dry forest, tropical shrubland, subtropical humid forest and subtropical steppe. These discrepancies could also be explained by the few observations we have in these areas (see table 4.1). Therefore, the number of samples considered in our study for these ecosystems might not be sufficient enough in order to estimate their forest biomass values. In addition, Yong forest biomass map has few calibration data in dry areas with low vegetation cover (e.g. shrubland, subtropical steppe, tropical dry forest) for the South American region (Yong *et al.*, 2014). Finally, Avitabile *et al.* (2011) argued that IPCC tier 1 estimates tends to overestimate biomass values for Ugandan forest compared to country-specific field data. This finding could also justify the discrepancies found in South America.

4.2.2. Comparison of carbon losses estimates with other studies

Table 4.2 compares the EF estimates per driver from our study to the ones provided by the IPCC Guidelines (2006). As we expected, the table illustrates that our study underestimates, in general, the EF estimates when one compares our results with the IPCC (2006) estimates. Our EF estimates are, in average, 98%, 307%, 1650%, 1500%, 55%, 423%, 1600% and 230% lower than the IPCC estimates for tropical rainforest, tropical moist deciduous forest, tropical dry forest, tropical shrubland, tropical mountain systems, subtropical humid forest, subtropical steppe and the temperate mountain systems ecozones, respectively.

Table 4.2: EF estimates per driver in different ecozones from our study and the IPCC AFOLU Guidelines (2006) in South America.

Domain	Ecological zone	Driver	EFs (MgC.ha^{-1}) from IPCC (2006)	EFs (MgC.ha^{-1}) from this study
Tropical	Tropical rainforest	Crop agriculture	150	98.49
		Pasture		76.09
		Tree crops		81.43
		Mixed agriculture		31.64
		Other land use		54.48
		Mining		39.2
		Infrastructure		121.68
		Water		121.68
	Tropical moist deciduous forest	Crop agriculture	110	28.84
		Pasture		22.76
		Tree crops		27.84
		Mixed agriculture		16.64
		Other land use		14.85
		Mining		NA
		Infrastructure		37.98
		Water		37.98
	Tropical dry forest	*Crop agriculture*	*105*	*8.69*
		Pasture		*0.69*
		Tree crops		*NA*
		Mixed agriculture		*1.97*
		Other land use		*0.87*
		Mining		*NA*
		Infrastructure		*11.64*
		Water		*11.64*
	Tropical shrubland	*Crop agriculture*	*40*	*NA*
		Pasture		*2.37*
		Tree crops		*NA*
		Mixed agriculture		*NA*
		Other land use		*NA*
		Mining		*Na*
		Infrastructure		*NA*
		Water		*NA*
	Tropical mountain systems	Crop agriculture	115	91.2
		Pasture		64.88
		Tree crops		44.85
		Mixed agriculture		28.16
		Other land use		45.61
		Mining		96.86
		Infrastructure		107.8
		Water		107.8

These discrepancies have been already explained in the previous section and are mainly related to the presence of both forest and non-forest polygons in a large number of pixels in the forest biomass map as well as the few number of observations in some ecozones and the few calibration data for the forest biomass map in dry areas. In addition, the discrepancies between the IPCC AFOLU Guidelines estimates and our study can also be explained by the difference in the estimations of biomass left (biomass $_{after}$) in a site after a deforestation event. For the IPCC estimates, it is assumed that all biomass is cleared when preparing a site for non-forest land uses, thus, the default for biomass$_{after}$ is 0 MgC ha^{-1} (IPCC, 2006). Conversely, our study aimed to estimate the "true" biomass$_{after}$ values. Indeed, depending on the forest conversion type (e.g. agriculture, pasture, other land use), the biomass$_{after}$ values might differ, in particular whether there are woody elements left on a specific deforested site or not. Finally, the estimates of EFs show large relative error ranges which could also be explained by the uncertainties in the Yong biomass map (figure 4.2).

Table 4.2: (Continued)

Domain	Ecological zone	Driver	EFs (MgC.ha^{-1}) from IPCC (2006)	EFs (MgC.ha^{-1}) from this study
Subtropical	Subtropical humid forest	Crop agriculture	110	5.92
		Pasture		14.06
		Tree crops		1.29
		Mixed agriculture		4.08
		Other land use		31.11
		Mining		NA
		Infrastructure		42.01
		Water		42.01
	Subtropical steppe	*Crop agriculture*	*40*	*NA*
		Pasture		*0.27*
		Tree crops		*NA*
		Mixed agriculture		*NA*
		Other land use		*0.49*
		Mining		*NA*
		Infrastructure		*NA*
		Water		*NA*
Temperate	Temperate mountain systems	Crop agriculture	115	NA
		Pasture		NA
		Tree crops		NA
		Mixed agriculture		NA
		Other land use		35.15
		Mining		NA
		Infrastructure		NA
		Water		NA

Table 4.3 illustrates the comparison of our estimates of carbon losses during the period 1990-2000 to a recent carbon emissions from tropical deforestation studiy by Achard *et al.* (2014) and the FAO estimates (FAO, 2010). Our continental estimates are lower than the estimates from Achard *et al.* (2014) and FAO (2010) studies (table 4.3). Although our sampling approach is similar to the study carried out by Achard *et al.* (2014), their approach seems to vary widely from our study. First, Achard *et al.* (2014) used Baccini and Saatchi forest biomass maps while we used the Yong forest map. The latest map results in a fusion between

Baccini and Saatchi map and it shows a better accuracy of regional biomass estimates (Yong *et al.*, 2014). Moreover, both Achard and FAO studies used $biomass_{after}$ values equal to zero while our study intends to estimate the "true" biomass left after deforestation event if one considers that the $biomass_{after}$ values differ per driver, in particular when there are still woody elements left in a deforested site. In addition, the FAO study also includes the carbon losses from forest degradation (FAO, 2010) which is not considered in our study, unless deforestation is following deforestation.

We also compare our results for the period 2000-2005 with the same studies mentioned in the previous paragraph and with two recent other estimates of carbon emissions from tropical deforestation by Wood Hole Research Centre (WHRC) (Baccini *et al.*, 2012) and WinRock International (Harris *et al.*, 2012) as well (table 4.3). Similar to the period 1990-2000, our annual carbon losses estimates are lower than the four other studies considered here. Besides the differences already mentioned in the previous paragraph between our study and Achard/FAO studies, these two studies cover the complete decade while our study covers only the first half of the 2000s, i.e. from year 2000 to year 2005. In addition, Achard *et al.* (2014) state that the spatial information from our sampling design has a much higher spatial detail compare to the one used in Baccini and Harris studies. In addition, Grainger (2008) states that the estimates described in the FRA 2010 are derived from national forest inventories and the use of national statistics is known to be limited in terms of data quality and consistency between countries. Finally, all the studies analysed the carbon losses in both Central and South America, while our study covers only South America.

Table 4.3: Annual carbon losses from gross loss of tropical forest cover for periods 1990-2000 and 2000-2005 in South America (values in $MtC.yr^{-1}$)

	Annual carbon losses ($MtC.yr^{-1}$)
Period 1990-2000	
Our study with Ecozone/Yong	195
Achard *et al.* (2014) with average Baccini/Saatchi	443.4
FAO (2010)	357.7
Period 2000-2005	
Our study with Ecozone/Yong	246
Achard *et al.* (2014) with average Baccini/Saatchi for the period 2000-2010	464.8
FAO (2010) for the period 2000-2010	340.1
Baccini *et al.* (2012)	470
Harris *et al.* (2012)	440

Furthermore, we want to compare our annual carbon losses per driver for the two periods with other studies. We do the comparison of our result with a study carried out by the WHRC (Houghton, 2012). However, we find it hard to do a realistic comparison between the two studies because the respective drivers' classification systems differ widely. Only the definitions of pasture seem to be quite similar in the two studies, therefore we find it reasonable to compare annual carbon losses from pasture expansion. Our estimate for pasture expansion is slightly higher than the estimates from Houghton study. Houghton *et al.* (2012), showed that forest conversion to pasture emitted 130 $MtC.yr^{-1}$ for 1990-2000 while our study showed a carbon loss value around 160 $MtC.yr^{-1}$ for the 1990-2005 time period. In addition, the proportion of pasture expansion in our study (75%) is much higher than the one found on Houghton study (25%). It was also interesting to see that crop agriculture and pasture

emissions have continued to grow between the two decades in our study. This is supported by Tubiello *et al.* (2015) study which analysed the contribution of AFOLU activities to global warming at global level. They highlighted that agriculture emissions have continued to grow, at roughly 1% annually, and remained larger than the land use sector from 1990 to 2012.

4.2.3. Spatial patterns of carbon losses

Our results showed that there are spatial and temporal patterns of carbon losses from deforestation. We have shown that the main area of carbon losses in both periods was in the so called 'arc of deforestation' of the Brazilian Amazon. This is in line with Achard *et al.* (2014) who have shown similar outcomes. We also pointed out two other hot-spots of carbon emissions in the area of the Colombian Amazon and in the region of Santa-Cruz. In addition, Achard *et al.* (2014) study has not described the proportions of carbon losses per driver whilst our study depicted that carbon losses are mainly driven by pasture and crop agriculture expansions in South America. Theses drivers showed new hotspots of deforestation between the 1990s and the 2000s mainly located in the amazon rainforest, particularly for pasture. This is in line with the increase of carbon losses for pasture and crop agriculture between the two time periods. There is a higher loss of biomass when deforestation events occur in intact tropical rainforest ecosystem than in already degraded ecosystems.

Chapter 5. Conclusions and recommendations

5.1. Conclusions

The work presented in this thesis aimed at answering two main questions: *How global land cover datasets can support the quantification and assessment of deforestation drivers in REDD+ countries?*; and, *How can gross carbon emissions per deforestation driver be estimated by using global forest biomass maps and sample-based driver data in the pan-tropical region countries?*

As explained in chapter 3, our study assessed three different global land cover maps against reference data for deforestation drivers' classification both in Africa and South America. Overall, global land cover maps showed potential opportunities for deforestation drivers' analysis. Although our study showed limitations of the MODIS and GLC-SHARE datasets to clearly discriminate deforestation drivers in Africa, the CCI-LC products depicted promising results. The latest products have proven to be useful for classifying agriculture driver class in both Africa and South America. In the African continent, the user can expect to classify accurately all areas that actually represent agriculture on the ground. However, due to its high commission error, our study demonstrated that one will likely overmap this class with the CCI-LC datasets. Like in Africa, the CCI-LC maps had high producer accuracies, however they also showed high user accuracies for the agriculture class. Therefore, overmapping for the agriculture class will be much lower in South America than in Africa. Additionally, our study showed another possible use of the CCI global land cover map in South America. Other land use class had high commission errors which were most of the time confused with the agriculture class. However, in the reference data, some polygons have been classified as other land use by the interpreter, although they probably could have been classified as agriculture. Therefore, one can argue that the CCI-LC maps could be used to check whether one polygon has been correctly classified as other land use or should, in fact, be labelled as agriculture class. In conclusion, the CCI-LC maps could provide an alternative to fill the gaps in the deforestation drivers' analysis but also improve the current drivers' classification, in particular in South America.

In this study, we also performed carbon losses estimates per driver in South America for the 1990-2005 time period integrating sampled-based driver data with wall-to-wall biomass data i.e. Yong *et al.* (2014) forest biomass map. First of all, we compared our results of forest biomass estimates with IPCC (2006) estimates. Our results demonstrated discrepancies between the two studies. Our approach seems to have a tendency to under-estimate the forest biomass with coarse forest biomass maps. Furthermore, we compared the EF estimates from our study with the IPCC estimates. Again, our study showed lower estimates than the IPCC estimates. This might be explained by the different approaches used by the two studies. For the IPCC estimates, it is assumed that all biomass is cleared while we presumed that there is biomass left after a deforestation event in a specific site. Additionally, our validation method has proven that the Yong global forest biomass map tends to under-estimate carbon stocks compared to reference data when one uses the average biomass values at ecosystem level. This could, therefore, justify the discrepancies between our study and IPCC estimates. Third, we analysed the annual carbon losses from deforestation at continental scale and compared our results with other studies. The comparison depicted that our study under-estimated the annual carbon losses in South America. Again, this could be explained by the fact that our

approach differs widely from the other studies in terms of forest biomass map used, EF estimates method, and the time period considered. In summary, our study showed opportunities to improve tier 1 GHG emission factors for deforestation by using global forest biomass maps. In addition, our results demonstrated the importance of carbon losses from forest in tropics, in particular from pasture and crop agriculture expansion. These results are, therefore, useful to further inform the current climate policy debate on land use change, suggesting that more efforts should be directed to further explore options for climate change mitigation in the AFOLU sector (Tubiello *et al.*, 2015).

5.2. Recommendations

Overall, this analysis has proven that the coarse resolution of the global land cover maps is a limitation for deforestation drivers' classification whilst also providing some opportunities. However, this may still be a matter of further investigation. First, one could investigate other land cover products currently available. For instance, the discrete SERENA land cover product (Blanco *et al.*, 2013) for Latin America and the Caribbean (LAC) for the year 2008 with a 500m resolution proved to be quite accurate which, therefore, could eventually improve the deforestation drivers analysis. Furthermore, in this study, we decided to aggregate driver classes into four main classes (e.g. agriculture, other land use, water and infrastructure) in order to simplify our assessment. However, it would be interesting to divide these classes according to the classification provided in table 2.3. This could allow us to see whether the confusion in one aggregated class comes from a specific sub-class or not. Finally, the driver classification in the reference data (deforestation drivers' classification with visual assessment) has been performed using high-resolution datasets (e.g. Landsat with a 30m resolution), whilst our driver's classification was performed using global land cover maps with coarse resolution. In this situation, Boschetti *et al.* (2004) recommended to use the 'Pareto Boundary' method which allows us to determine the maximum user and producer's accuracy values that could be attained jointly by a low-resolution map. This method could help us to understand whether the limited accuracy of a low spatial resolution map is given by poor performance of the classification algorithm or by the low resolution of the remotely sensed data, which had been classified (Boschetti *et al.*, 2004).

During the implementation of the carbon emissions analysis presented in this thesis, the authors faced some challenges. We came across several questions, thus, further research on the carbon emissions analysis might be needed to improve our approach. First of all, we decided to subset our samples per ecozone at a continental scale (see figure 2.6). Therefore, our study assumed that a land use' biomass value, i.e. forest, crop agriculture, pasture, in a specific ecozone is comparable all over the continent. However, this assumption could be criticized because within an ecozone there are areas much dryer than others and vice-versa. Therefore, the authors propose to create sub-ecozones at a regional scale in order to decrease the uncertainties of our estimates. Furthermore, our driver classification for the EF estimates did not distinguish patches with either woody or non-woody elements. Therefore, one could think about creating for each deforestation's driver class, a class including the areas with woody elements and another class with non-woody areas. Obviously, this would help us to optimize our approach. Our study also showed that our method underestimates, in general, the biomass values and emission factors. This was clearly confirmed by our validation method using high resolution carbon stock maps (Asner *et al.*, 2014; 2012). One of the reasons of these discrepancies was related to the difference between polygon minimum mapping unit (MMU) area and pixel size of the forest biomass map. Therefore, to overcome this issue, we recommend to remove the polygons with a MMU lower than the pixel size and

the polygons mixed with other type of land use (e.g. forest and non-forest) in one pixel. Additionally, it would be relevant to use the bias ‘assessment of the EF estimates from the validation method in order to correct our estimation. Finally, our method has shown limitations due to the uncertainty in the spatial distribution of tropical forest biomass from the current global forest biomass maps, in particular in dry areas with low vegetation cover where calibration data are missing. That is why Mitchard *et al.* (2013) and Avitabile *et al.* (2011) state that the future priorities for the reduction in uncertainties in estimates of carbon emissions from land-use changes in the tropics lie in the improvement of regional forest inventories for assessing carbon content at a local scale for all kind of ecosystems. The two new global biomass products of Baccini (30m resolution) and Saatchi (100m resolution) announced to be released soon would eventually decrease these uncertainties, in particular, the Saatchi map which estimates the wood density. It would, therefore, be interesting to test our method using these two new products.

References

Achard, F., 1Beuchle, R.,Mayaux, P., Stibig, H.J., Bodart, C., Brink, A., Carboni, S., Desclée, B., Donnay, F., Eva, H.D., Lupi, A., Raši, R., Seliger, R. and Simonetti, D. (2014). "Determination of tropical deforestation rates and related carbon losses from 1990 to 2010." Global Change Biology 20: 2540–2554.

Anderson, J. F., Hardy, E. E., Roach, J. T., & Witmer, R. E. (1976). A land use and land cover classification system for use with remote sensor data. U.S. Geological Survey Professional Paper 964, U.S. Geological Survey, Washington, DC, 28pp.

Asner, G. P. K., D., Martin, R., Tupayachi, R., Anderson, C., Mascaro, J., Sinca, F., Chadwick, K.D, Sousan, S., Higgins, M., Farfan, W., Silman, M.R, Augusto, W., León, L., and Palomino, A.F,N. (2014). "Targeted carbon conservation at national scales with high-resolution monitoring." PNAS.

Asner, G. P. C., J. K., Mascaro, J., Galindo Garcia, G. A. , Chadwick, K. D. , Navarrete Encinales, D. A., Paez-Acosta, G., Cabrera Montenegro, E., Kennedy-Bowdoin, T, Duque, A., Balaji, A., von Hildebrand, P., MaatougL., Phillips, J. F., Bernal, Yepes Quintero, A. P., Knapp, D. E. , Garcia Davila, D. E., Jacobson, J. and Ordonez, D. E. (2012). "High-resolution mapping of forest carbon stocks in the Colombian Amazon." Biogeosciences (9): 2683–2696.

Avitabile, V., Herold, V., Henry, M. and Schmullius, C. (2011). "Mapping biomass with remote sensing: a comparison of methods for the case study of Uganda." Carbon Balance and Management 6(7).

Baccini, A., Goetz, S. J., Walker, W. S., Laporte, N. T., Sun, M., Sulla-Menashe, D., Hackler, J., Beck, P. S. A., Dubayah, R., Friedl, M. A., Samanta, S. and Houghton, R. A. (2012). "Estimated carbon dioxide emissions from tropical deforestation improved by carbon-density maps." Nature Climate Change 1354.

Blanco, *et al.* (2013). "A land cover map of Latin America and the Caribbean in the framework of the SERENA project " Remote Sensing of Environment 132: 13-31.

Boucher, D., Elias, P., Lininger, K., May-Tobin, C., Roquemore, S. and Saxon E. (2011). "The Root of the Problem: What 's Driving Tropical Deforestation Today?" Union of Concerned Scientists. Cambridge, Massachusetts.

Boschetti, L., Flasse, S.P., Brivio, P.A. (2004). "Analysis of the conflict between omission and commission in low spatial resolution dichotomic thematic products: The Pareto Boundary." Remote Sensing of Environment 91: 280-292.

Canadell, J., Le Quere, C., Raupach, MR., Field, CB., Buitenhuis, ET., Ciais, P., Conway, TJ., Gillett, NP., Houghton, RA. and Marland, G. (2007). "Contributions to accelerating atmospheric CO2 growth from economic activity, carbon intensity, and efficiency of natural sinks." Proceedings of the National Academy of Sciences 104: 18866-18870.

Chave, J. *et al*. (2005). "Tree allometry and improved estimation of carbon stocks and balance in tropical forests." Oecologia 145, 87-99.

Defries, R. S., Rudel, T., Uriarte, M. and Hansen. M. (2010). "Deforestation driven by urban population growth and agricultural trade in the twenty-first century." Nature Geoscience 3: 178-181.

FAO (2012). "Global ecological zones for FAO forest reporting: 2010 Update". FAO Forest Resources Assessment Working Paper 179. Rome, Italy.

FAO (2010). "Global Forest Resources Assessment 2010." FAO Forestry Paper 163.

FAO (2009). "The 2010 Global Forest Resources Assessment Remote Sensing Survey: an outline of the objectives, data, methods and approach. Forest." Resources Assessment Working Paper 155. Published by FAO with FRA RSS partners, Rome, 2009.

Geist, H., Lambin, E. (2002). "Proximate causes and underlying driving forces of tropical deforestation." BioScience 52: 143–150.

GOFC-GOLD (2010). "Sourcebook of Methods and Procedures for Monitoring and Reporting Anthropogenic Greenhouse Gas Emissions and Removals Caused by Deforestation, Gains and Losses of Carbon Stocks in Forests Remaining Forests, and Forestation." Global Observations of Forest and Land Cover Dynamics Project Office, AB, Canada.

GOFC-GOLD (2009). "Sourcebook of Methods and Procedures for Monitoring and Reporting Anthropogenic Greenhouse Gas Emissions and Removals Caused by Deforestation, Gains and Losses of Carbon Stocks in Forests Remaining Forests, and Forestation." Version COP15-1 edition.

Grainger, A. (2008). "Difficulties in tracking the long-term global trend in tropical forest area." Proceedings of the National Academy of Sciences, 105, 818–823.

Harris, N. L., Brown, S., Hagen, S.C, Saatchi, S.S, Petrova,S., Salas, W., Hansen, M.C, Potapov, P.V, and Lotsch, A. (2012). "Baseline Map of Carbon Emissions from Deforestation in Tropical Regions." Science 336: 1573.

Herold, M., Román-Cuesta, R.M., Mollicone, D., Hirata, Y., Van Laak, P., Asner, G.P., Carlos Souza, C., Skutsch, M., Avitabile, V., and MacDicken, K. (2011). "Options for monitoring and estimating historical carbon emissions from forest degradation in the context of REDD+." Carbon Balance and Management 6(13).

Herold, M., Mayaux , P., Woodcock, C.E., Baccini, A., Schmullius, C. (2008). "Some challenges in global land cover mapping: An assessment of agreement and accuracy in existing 1 km datasets." Remote Sensing of Environment 112: 2538–2556.

Hosonuma, N., Herold, M., De Sy, V., De Fries, R-S., Brockhaus, M., Verchot, L., Angelsen, A. and Romijn, E. (2012). "An assessment of deforestation and forest degradation drivers in developing countries." Environmental Research Letters 7: 12.

Houghton, R. A. (2012). "Carbon emissions and the drivers of deforestation and forest degradation in the tropics." Current Opinion in Environmental Sustainability 4: 597-603.

Houghton, R. A., House, J. I., Pongratz, J., van der Werf, G. R., DeFries, R. S., Hansen, M. C., Le Quere, C. and Ramankutty, N. (2012). "Carbon emissions from land use and land-cover change." Biogeosciences 9(12): 5125-5142.

IPCC (2007). "IPCC Fourth Assessment Report: Climate Change 2007." IPCC, Geneva, Switzerland: pp 104.

IPCC. (2006). "IPCC Guidelines for National Greenhouse Gas Inventories, Prepared by the National Greenhouse Gas Inventories Programme". IPCC 2006.

IPCC. (2003). "Good Practice Guidance for Land Use, Land-Use Change and Forestry". Geneva; 2003.

Kissinger, G., Herold, M. and De Sy, V. (2012). "Drivers of Deforestation and Forest Degradation: A Synthesis Report for REDD+ Policymakers." Lexeme Consulting, Vancouver Canada, August 2012.

Kuenzer, C., Leinenkugel, P., Vollmuth, M. and Dech, S. (2014). "Comparing global land-cover products – implications for geoscience applications: an investigation for the trans-boundary Mekong Basin." International Journal of Remote Sensing 35(8): 2752-2779.

MEA (2005). "Ecosystems and Human Well-being: Synthesis." Island Press, Washington, DC.

Mitchard, ETA., Saatchi, S.S., Baccini, A., Asner, G.P., Goetz, S.J., Harris, N.L, Brown, S. (2013). "Uncertainty in the spatial distribution of tropical forest biomass: a comparison of pan-tropical maps". Carbon Balance and Management, 8, 10.

Morton, D.C., DeFries, R.S., Olivier, J.G.J., Kasibhatla, P.S., Jackson, R.B, Collatz, G.J., Randerson, J.T. (2009). "CO2 emissions from forest loss". Nature Geosciences 2:737–738.

Potere, D., A. Schneider. (2007). "A critical look at representations of urban areas in global maps". GeoJournal 69:55-80.

R Development Core Team. (2013). “R: A Language and Environment for Statistical Computing (version 3.02)”. R Development Core Team. http://www.R-project.org/.

Rademaekers, K., Eichler, L., Berg, J., Obersteiner, M. and Havlik P. (2010). "Study on the evolution of some deforestation drivers and their potential impacts on the costs of an avoiding deforestation scheme." Prepared for the European Commission by ECORYS and IIASA. Rotterdam, Netherlands.

Rudel, T. K., Schneider, L., Uriarte, M., Turner, B.L., DeFries, R., Lawrence, D., Geoghegan, J., Hecht, S., Ickowitz, A. and Lambin, E.F. (2009). "Agricultural intensification and changes in cultivated areas, 1970–2005." Proceedings of the National Academy of Sciences 106: 20675–20680.

Saatchi, S.S., Harris, N.L., Brown,S., Lefsky, M., Mitchard, E.T.A, Salas, W., Zutta, B.R., Buermann, W., Lewis, S.L., Hagen, S., Petrova, S., White, L. Silman, M.and Morel, A. (2011). "Benchmark map of forest carbon stocks in tropical regions across three continents." Proceedings of the National Academy of Sciences 108(24): 9899-9904.

Salimon, C. I., Putz, F.E, Menezes-Filho, L., Anderson, A., Silveira, M., Brown, I.F., Oliveira, L.C. (2011). "Estimating state-wide biomass carbon stocks for a REDD plan in Acre, Brazil." Forest Ecology and Management 262: 555-560.

Tubiello, F. *et al.* (2015). "The Contribution of Agriculture, Forestry and other Land Use activities to Global Warming, 1990–2012." Global Change Biology.

UNFCCC, 2009. Methodological guidance for activities relating to reducing emissions from deforestation and forest degradation and the role of conservation, sustainable management of forests and enhancement of forest carbon stocks in developing countries. UNFCCC Secretariat, Bonn, Germany 2009.

UNFCCC, 2010. Outcome of the work of the Ad Hoc Working Group on long-term Cooperative Action under the Convention - C. Policy approaches and positive incentives on issues relating to reducing emissions from deforestation and forest degradation in developing countries. UNFCCC Secretariat, Bonn, Germany 2010.

Yong, G., Avitabile, V., Heuvelink, G.B.M, Wanga, J., Herold, M. (2014). "Fusion of pan-tropical biomass maps using weighted averaging and regional calibration data." International Journal of Applied Earth Observation and Geoinformation 31: 13-24.

Wickham, J. D., Stehman, S. V., Fry, J. A., Smith, J. H., & Homer, C. G. (2010). Thematic accuracy of the 2001 National Land-Cover Data for the conterminous United States. Remote Sensing of Environment 114, 1286-1296.

Annexes

Annexe 1: FAO Land Cover Classification System legend with corresponding classes from individual global legends. Source: adapted from Kuenzer *et al.* (2014)

Drivers classification		**FAO LUCS**		**FAO LCCS**		**CCI-LC**		**GLC-SHARE**		**MOD500**	
Class	Generalized class description	Class	Generalized class description	Class	Generalized class description	Class	Class description	Class	Class description	Class	Class description
100	Forest	11	Forest	1	Evergreen needle leaf trees	70	Tree cover, needle leaved, evergreen, closed to open (>15%)			1	Evergreen needle leaf forest
				2	Evergreen broadleaf trees	50	Tree cover, broadleaved, evergreen, closed to open (>15%)			2	Evergreen broadleaf forest
				3	Deciduous needle leaf trees	80	Tree cover, needle leaved, deciduous, closed to open (>15%)			3	Deciduous needle leaf forest
				4	Deciduous broadleaf trees	60	Tree cover, broadleaved, deciduous, closed to open (>15%)			4	Deciduous broadleaf forest
				5	Mixed/other trees	90	Tree cover, mixed leaf type (broadleaved and needle leaved)	4	Tree covered areas	5	Mixed forest
										8	Woody savannahs
		12	Other wooded land			100	Mosaic tree and shrub (>50%)/ herbaceous cover (<50%)				
						110	Mosaic herbaceous cover (>50%)/ tree and shrub (<50%)			9	Savannahs
						160	Tree cover, flooded, fresh or brakish water				
						170	Tree cover, flooded, fresh or saline water	7	Mangroves		

Annexe 1: (Continued)

Drivers classification			FAO LUCS		FAO LCCS		CCI-LC		GLC-SHARE		MOD500	
Class	Generalized class description		Class	Generalized class description	Class	Generalized class description	Class	Class description	Class	Class description	Class	Class description
500	Other	520	13	Other land with tree cover	6	Shrubs	120	Shrubland	5	Shrubs Covered Areas	6	Closed shrublands
							150	Sparse vegetation (tree, shrub, herbaceous cover) (<15%)	8	Sparse vegetation	7	Open shrublands
		530	14	Grass and herbaceous cover			140	Lichens and mosses				
					7	Herbaceous vegetation	130	Grasslands	3	Grassland	10	Grasslands
		540	19	Wetlands	9	Other shrub/ herbaceous vegetation	180	Shrub or herbaceous cover, flooded, fresh/saline/brakish water	6	Herbaceous vegetation, aquatic or regularly flooded	11	Permanent wetlands
		510	17	Bare land	11	Snow and Ice	220	Permanent snow and ice	10	Snow and glaciers	15	Snow and ice
					12	Barren	200	Bare areas	9	Bare soil	16	Barren or sparsely vegetated
200	Agriculture		15	Agricultural crops	8	Cultivated and managed vegetation/ agriculture (incl. mixtures)	20	Cropland, irrigated or post-flooding	2	Cropland	12	Croplands
							10	Cropland, rainfed				
							30	Mosaic cropland (>50%)/ natural vegetation (tree, shrub, herbaceous cover) <50%)				
							40	Mosaic natural vegetation (tree, shrub, herbaceous cover) (>50%)/ crop land (<50%)				
											14	Cropland/natural vegetation mosaic

Annexe 1: (Continued)

Drivers classification		FAO LUCS		FAO LCCS		CCI-LC		GLC-SHARE		MOD500	
Class	Generalized class description	Class	Generalized class description	Class	Generalized class description	Class	Class description	Class	Class description	Class	Class description
300	Built-up	16	Built up habitation	10	Urban/ built-up	190	Urban areas	1	Artificial surfaces	13	Urban and built-up
600	Water	18	Water	13	Open water	210	Water bodies	11	Water bodies	0	Water